

# World Journal of *Gastroenterology*

*World J Gastroenterol* 2023 June 14; 29(22): 3385-3573



**REVIEW**

- 3385 Overview of current detection methods and microRNA potential in *Clostridioides difficile* infection screening  
*Bocchetti M, Ferraro MG, Melisi F, Grisolia P, Scrima M, Cossu AM, Yau TO*
- 3400 Epidemiology of small intestinal bacterial overgrowth  
*Efremova I, Maslennikov R, Poluektova E, Vasilieva E, Zharikov Y, Suslov A, Letyagina Y, Kozlov E, Levshina A, Ivashkin V*

**ORIGINAL ARTICLE****Basic Study**

- 3422 Mechanism of annexin A1/N-formylpeptide receptor regulation of macrophage function to inhibit hepatic stellate cell activation through Wnt/ $\beta$ -catenin pathway  
*Fan JH, Luo N, Liu GF, Xu XF, Li SQ, Lv XP*
- 3440 Study of the roles of caspase-3 and nuclear factor kappa B in myenteric neurons in a P2X7 receptor knockout mouse model of ulcerative colitis  
*Magalhães HIR, Machado FA, Souza RF, Caetano MAF, Figliuolo VR, Coutinho-Silva R, Castelucci P*
- 3469 Comparative analysis of the gut microbiota of wild adult rats from nine district areas in Hainan, China  
*Niu LN, Zhang GN, Xuan DD, Lin C, Lu Z, Cao PP, Chen SW, Zhang Y, Cui XJ, Hu SK*

**Case Control Study**

- 3482 Plasma exosomal hsa\_circ\_0079439 as a novel biomarker for early detection of gastric cancer  
*Li X, Lin YL, Shao JK, Wu XJ, Li X, Yao H, Shi FL, Li LS, Zhang WG, Chang ZY, Chai NL, Wang YL, Linghu EQ*

**Retrospective Cohort Study**

- 3497 Per-oral endoscopic myotomy is safe and effective for pediatric patients with achalasia: A long-term follow-up study  
*Bi YW, Lei X, Ru N, Li LS, Wang NJ, Zhang B, Yao Y, Linghu EQ, Chai NL*

**Retrospective Study**

- 3508 Efficacy and safety of modified tetracycline dosing in a quadruple therapy for *Helicobacter pylori*: A retrospective single center study  
*Sun YC, Zhu MJ, Chen XQ, Yue L, Zhao YR, Wang XJ, Kim JJ, Du Q, Hu WL*

**Observational Study**

- 3519 Pre-transjugular-intrahepatic-portosystemic-shunt measurement of hepatic venous pressure gradient and its clinical application: A comparison study  
*Wang XX, Yin XC, Gu LH, Guo HW, Cheng Y, Liu Y, Xiao JQ, Wang Y, Zhang W, Zou XP, Wang L, Zhang M, Zhu-Ge YZ, Zhang F*

- 3534** Difference and clinical value of metabolites in plasma and feces of patients with alcohol-related liver cirrhosis

*Xu YF, Hao YX, Ma L, Zhang MH, Niu XX, Li Y, Zhang YY, Liu TT, Han M, Yuan XX, Wan G, Xing HC*

**Prospective Study**

- 3548** Prospective study comparing hepatic steatosis assessment by magnetic resonance imaging and four ultrasound methods in 105 successive patients

*Collin R, Magnin B, Gaillard C, Nicolas C, Abergel A, Buchard B*

**SCIENTOMETRICS**

- 3561** Research trends on artificial intelligence and endoscopy in digestive diseases: A bibliometric analysis from 1990 to 2022

*Du RC, Ouyang YB, Hu Y*

**ABOUT COVER**

Editorial Board Member of *World Journal of Gastroenterology*, Wolfgang Kreisel, MD, Emeritus Professor, Department of Medicine II, Gastroenterology, Hepatology, Endocrinology, and Infectious Diseases, Faculty of Medicine, Medical Center-University of Freiburg, Hugstetter Str. 55, Freiburg 79106, Germany. Wolfgang.Kreisel@uniklinik-freiburg.de

**AIMS AND SCOPE**

The primary aim of *World Journal of Gastroenterology* (WJG, *World J Gastroenterol*) is to provide scholars and readers from various fields of gastroenterology and hepatology with a platform to publish high-quality basic and clinical research articles and communicate their research findings online. WJG mainly publishes articles reporting research results and findings obtained in the field of gastroenterology and hepatology and covering a wide range of topics including gastroenterology, hepatology, gastrointestinal endoscopy, gastrointestinal surgery, gastrointestinal oncology, and pediatric gastroenterology.

**INDEXING/ABSTRACTING**

The WJG is now abstracted and indexed in Science Citation Index Expanded (SCIE, also known as SciSearch®), Current Contents/Clinical Medicine, Journal Citation Reports, Index Medicus, MEDLINE, PubMed, PubMed Central, Scopus, Reference Citation Analysis, China National Knowledge Infrastructure, China Science and Technology Journal Database, and Superstar Journals Database. The 2022 edition of Journal Citation Reports® cites the 2021 impact factor (IF) for WJG as 5.374; IF without journal self cites: 5.187; 5-year IF: 5.715; Journal Citation Indicator: 0.84; Ranking: 31 among 93 journals in gastroenterology and hepatology; and Quartile category: Q2. The WJG's CiteScore for 2021 is 8.1 and Scopus CiteScore rank 2021: Gastroenterology is 18/149.

**RESPONSIBLE EDITORS FOR THIS ISSUE**

Production Editor: *Hua-Ge Yu*; Production Department Director: *Xu Guo*; Editorial Office Director: *Jia-Ru Fan*.

**NAME OF JOURNAL**

*World Journal of Gastroenterology*

**ISSN**

ISSN 1007-9327 (print) ISSN 2219-2840 (online)

**LAUNCH DATE**

October 1, 1995

**FREQUENCY**

Weekly

**EDITORS-IN-CHIEF**

Andrzej S Tarnawski

**EDITORIAL BOARD MEMBERS**

<http://www.wjgnet.com/1007-9327/editorialboard.htm>

**PUBLICATION DATE**

June 14, 2023

**COPYRIGHT**

© 2023 Baishideng Publishing Group Inc

**INSTRUCTIONS TO AUTHORS**

<https://www.wjgnet.com/bpg/gerinfo/204>

**GUIDELINES FOR ETHICS DOCUMENTS**

<https://www.wjgnet.com/bpg/GerInfo/287>

**GUIDELINES FOR NON-NATIVE SPEAKERS OF ENGLISH**

<https://www.wjgnet.com/bpg/gerinfo/240>

**PUBLICATION ETHICS**

<https://www.wjgnet.com/bpg/GerInfo/288>

**PUBLICATION MISCONDUCT**

<https://www.wjgnet.com/bpg/gerinfo/208>

**ARTICLE PROCESSING CHARGE**

<https://www.wjgnet.com/bpg/gerinfo/242>

**STEPS FOR SUBMITTING MANUSCRIPTS**

<https://www.wjgnet.com/bpg/GerInfo/239>

**ONLINE SUBMISSION**

<https://www.f6publishing.com>

## Basic Study

# Study of the roles of caspase-3 and nuclear factor kappa B in myenteric neurons in a P2X7 receptor knockout mouse model of ulcerative colitis

Henrique Inhauser Riceti Magalhães, Felipe Alexandre Machado, Roberta Figueiroa Souza, Marcos Antônio Ferreira Caetano, Vanessa Ribeiro Figliuolo, Robson Coutinho-Silva, Patricia Castelucci

**Specialty type:** Anatomy and morphology

**Provenance and peer review:** Invited article; Externally peer reviewed.

**Peer-review model:** Single blind

**Peer-review report's scientific quality classification**

Grade A (Excellent): 0  
Grade B (Very good): B, B  
Grade C (Good): 0  
Grade D (Fair): 0  
Grade E (Poor): 0

**P-Reviewer:** Arslan M, Turkey; Pisani LF, Italy

**Received:** February 27, 2023

**Peer-review started:** February 27, 2023

**First decision:** April 3, 2023

**Revised:** April 25, 2023

**Accepted:** May 12, 2023

**Article in press:** May 12, 2023

**Published online:** June 14, 2023



**Henrique Inhauser Riceti Magalhães**, Department of Surgery, School of Veterinary Medicine and Animal Sciences, University of São Paulo, São Paulo 05508-270, Brazil

**Felipe Alexandre Machado, Roberta Figueiroa Souza, Marcos Antônio Ferreira Caetano, Patricia Castelucci**, Department of Anatomy, University of São Paulo, São Paulo 05508-000, Brazil

**Vanessa Ribeiro Figliuolo, Robson Coutinho-Silva**, Biophysics Institute Carlos Chagas Filho, Federal University of Rio de Janeiro, Rio de Janeiro 21941-902, Brazil

**Corresponding author:** Patricia Castelucci, MHS, PhD, Associate Professor, Associate Research Scientist, Lecturer, Department of Anatomy, University of São Paulo, 2415, Av. Dr Lineu Prestes, São Paulo 05508-000, Brazil. [pcastel@usp.br](mailto:pcastel@usp.br)

## Abstract

### BACKGROUND

The literature indicates that the enteric nervous system is affected in inflammatory bowel diseases (IBDs) and that the P2X7 receptor triggers neuronal death. However, the mechanism by which enteric neurons are lost in IBDs is unknown.

### AIM

To study the role of the caspase-3 and nuclear factor kappa B (NF- $\kappa$ B) pathways in myenteric neurons in a P2X7 receptor knockout (KO) mouse model of IBDs.

### METHODS

Forty male wild-type (WT) C57BL/6 and P2X7 receptor KO mice were euthanized 24 h or 4 d after colitis induction by 2,4,6-trinitrobenzene sulfonic acid (colitis group). Mice in the sham groups were injected with vehicle. The mice were divided into eight groups ( $n = 5$ ): The WT sham 24 h and 4 d groups, the WT colitis 24 h and 4 d groups, the KO sham 24 h and 4 d groups, and the KO colitis 24 h and 4 d groups. The disease activity index (DAI) was analyzed, the distal colon was collected for immunohistochemistry analyses, and immunofluorescence was performed to identify neurons immunoreactive (ir) for calretinin, P2X7 receptor, cleaved caspase-3, total caspase-3, phospho-NF- $\kappa$ B, and total NF- $\kappa$ B. We analyzed the number of calretinin-ir and P2X7 receptor-ir neurons per ganglion, the neuronal profile area ( $\mu\text{m}^2$ ), and corrected total cell fluorescence (CTCF).

## RESULTS

Cells double labeled for calretinin and P2X7 receptor, cleaved caspase-3, total caspase-3, phospho-NF- $\kappa$ B, or total NF- $\kappa$ B were observed in the WT colitis 24 h and 4 d groups. The number of calretinin-ir neurons per ganglion was decreased in the WT colitis 24 h and 4 d groups compared to the WT sham 24 h and 4 d groups, respectively ( $2.10 \pm 0.13$  vs  $3.33 \pm 0.17$ ,  $P < 0.001$ ;  $2.92 \pm 0.12$  vs  $3.70 \pm 0.11$ ,  $P < 0.05$ ), but was not significantly different between the KO groups. The calretinin-ir neuronal profile area was increased in the WT colitis 24 h group compared to the WT sham 24 h group ( $312.60 \pm 7.85$  vs  $278.41 \pm 6.65$ ,  $P < 0.05$ ), and the nuclear profile area was decreased in the WT colitis 4 d group compared to the WT sham 4 d group ( $104.63 \pm 2.49$  vs  $117.41 \pm 1.14$ ,  $P < 0.01$ ). The number of P2X7 receptor-ir neurons per ganglion was decreased in the WT colitis 24 h and 4 d groups compared to the WT sham 24 h and 4 d groups, respectively ( $19.49 \pm 0.35$  vs  $22.21 \pm 0.18$ ,  $P < 0.001$ ;  $20.35 \pm 0.14$  vs  $22.75 \pm 0.51$ ,  $P < 0.001$ ), and no P2X7 receptor-ir neurons were observed in the KO groups. Myenteric neurons showed ultrastructural changes in the WT colitis 24 h and 4 d groups and in the KO colitis 24 h group. The cleaved caspase-3 CTCF was increased in the WT colitis 24 h and 4 d groups compared to the WT sham 24 h and 4 d groups, respectively ( $485949 \pm 14140$  vs  $371371 \pm 16426$ ,  $P < 0.001$ ;  $480381 \pm 11336$  vs  $378365 \pm 4053$ ,  $P < 0.001$ ), but was not significantly different between the KO groups. The total caspase-3 CTCF, phospho-NF- $\kappa$ B CTCF, and total NF- $\kappa$ B CTCF were not significantly different among the groups. The DAI was recovered in the KO groups. Furthermore, we demonstrated that the absence of the P2X7 receptor attenuated inflammatory infiltration, tissue damage, collagen deposition, and the decrease in the number of goblet cells in the distal colon.

## CONCLUSION

Ulcerative colitis affects myenteric neurons in WT mice but has a weaker effect in P2X7 receptor KO mice, and neuronal death may be associated with P2X7 receptor-mediated caspase-3 activation. The P2X7 receptor can be a therapeutic target for IBDs.

**Key Words:** Cell death; Enteric nervous system; Gastroenterology; Inflammatory bowel diseases; P2X7 receptor; Purinergic signaling

©The Author(s) 2023. Published by Baishideng Publishing Group Inc. All rights reserved.

**Core Tip:** In the present study, we compared pathological changes resulting from 2,4,6-trinitrobenzene sulfonic acid (TNBS)-induced colitis at two different time points after colitis induction. At both 24 h and four days post-inflammatory induction, there was a decrease in the number of myenteric neurons in the wild-type groups but not in the knockout groups. Morphometric and ultrastructural changes were also observed. In addition, our results confirm that neuronal death mediated by caspase-3 activation is related to purinergic signaling *via* the P2X7 receptor in the myenteric plexus of mice with TNBS-induced colitis.

**Citation:** Magalhães HIR, Machado FA, Souza RF, Caetano MAF, Figliuolo VR, Coutinho-Silva R, Castelucci P. Study of the roles of caspase-3 and nuclear factor kappa B in myenteric neurons in a P2X7 receptor knockout mouse model of ulcerative colitis. *World J Gastroenterol* 2023; 29(22): 3440-3468

**URL:** <https://www.wjgnet.com/1007-9327/full/v29/i22/3440.htm>

**DOI:** <https://dx.doi.org/10.3748/wjg.v29.i22.3440>

## INTRODUCTION

According to Martin[1] and Kanduc *et al*[2], cells usually die by apoptosis or necrosis, each of which has distinct microscopic and biochemical characteristics. In the process of apoptosis, the death stimulus activates a cascade of events that orchestrate the destruction of the cell under both physiological and pathological conditions[3,4]. Apoptosis is a programmed, dynamic, and energy-demanding process[5] and can occur in areas not severely affected by acute injury[4]. The cell volume decreases, the cytoplasm and nucleus become condensed, cytoskeletal proteins are cleaved, and apoptotic bodies form[3-10]. On the other hand, in necrosis, an unintentional, passive, and pathological process, the death stimulus itself causes the death of the cell[3-5] and affects groups of cells across tissues[8]. Cells and their organelles swell, and disruption of cytoplasmic membranes and degradation of deoxyribonucleic acid (DNA) occur[1,5,6,8,11,12]. Nuclear dissolution results from autolysis[5]. Activation of caspases is the main mechanism underlying cell death[3,7,8,13-15].

Studies of the central nervous system have shown that degeneration of neurons can occur through different pathways, including apoptotic pathways[4,8,16,17]. In acute neurological diseases, cell loss can occur either through necrosis or apoptosis[18-23], whereas in chronic neurodegenerative diseases, caspase-mediated pathways play dominant roles in mediating neuronal dysfunction and death[4,8,21,24-28]. In addition, loss of enteric nervous system (ENS) neurons has been demonstrated to occur after intestinal ischemia and reperfusion[29-34] and in experimental colitis[35-40].

The unexpected ability of certain cells to survive the activation of caspases[41-43] demonstrates the remarkable plasticity of cell death programs and suggests that the action of these proteases alone is not sufficient to cause cell loss[3]. Cell death, including that of enteric neurons, can occur through several caspase-independent pathways[3,44-47], and the signals that result in nonapoptotic cell death can come from numerous membrane receptors associated, directly or indirectly, or not with the activation of caspases themselves[3]. The P2X7 receptor is an important inducer of cell death[37,47-55] and is strongly associated with both the activation of caspases and the release and regulation of proinflammatory cytokines and transcription factors such as nuclear factor kappa B (NF- $\kappa$ B)[47,50,52,56-59].

Thus, improving the understanding of the cellular and molecular basis of neuronal death can aid in the identification and development of specific therapeutic strategies[8]. However, studies on the mechanisms underlying the death of enteric neurons, especially the role of the P2X7 receptor as an inducer of the death of these neurons in inflammatory bowel diseases (IBDs), are still lacking[37-40,51,52,60-63].

We aimed to study the roles of the caspase-3 and NF- $\kappa$ B pathways in myenteric neurons of the distal colon in a P2X7 receptor knockout (KO) mouse model of ulcerative colitis. The effects of colitis on calretinin neurons and intestinal tissue were analyzed by immunohistochemistry and histology, respectively.

## MATERIALS AND METHODS

The animal experiments were conducted in accordance with the current regulations of the Ethics Committee on Animal Use of the Institute of Biomedical Sciences of the University of São Paulo. In addition, all procedures were approved by the Ethics Committee on Animal Use of the School of Veterinary Medicine and Animal Science of the University of São Paulo (No. 2841270120) and by the Ethics Committee on Animal Use of the Institute of Biomedical Sciences of the University of São Paulo (No. 2372300921).

Forty eight-week-old male C57BL/6 mice weighing 20 g to 30 g, *i.e.*, 20 wild-type (WT) and 20 P2X7 receptor KO (P2X7<sup>-/-</sup>, P2X7 KO) animals, were used. The animal protocol was designed to minimize pain and discomfort in the animals. The mice were provided water and food *ad libitum* in ventilated cages on a 12 h light/dark cycle at a controlled temperature (21 °C). The animals were divided into eight groups of five animals each ( $n = 5$ ): The WT sham 24 h and 4 days (d) groups, the WT colitis 24 h and 4 d groups, the KO sham 24 h and 4 d groups, and the KO colitis 24 h and 4 d groups.

### Ulcerative colitis model

Mice were anesthetized *via* subcutaneous administration of an anesthetic solution of 2% xylazine (5 mg/kg) and 10% ketamine (80 mg/kg). Then, the animals in the colitis groups (WT colitis 24 h, KO colitis 24 h, WT colitis 4 d, and KO colitis 4 d groups) were given an intrarectal injection of 100  $\mu$ L of 2,4,6-trinitrobenzene sulfonic acid (TNBS, Sigma, United States of America) diluted to 1.5% in 35.0% ethanol (Synth, Brazil). The solution was deposited directly in the lumen of the large intestine with a four-centimeter-long polypropylene cannula. The animals in the sham groups (WT sham 24 h, KO sham 24 h, WT sham 4 d, and KO sham 4 d groups) received 100  $\mu$ L of 35% ethanol (vehicle) by the same method. The animals were euthanized by administration of an overdose of anesthetic solution 24 h or four days after the procedures. After the abdominal cavity of each animal was opened, the large intestine was identified, dissected, collected, and measured. The tissue was then sectioned along the mesenteric margin, and its contents were flushed with 0.01 M phosphate buffered saline (PBS) (pH 7.1-7.2). Only the distal colon was used for the analyses.

**Disease activity index:** Changes in weight, stool consistency, and the presence of blood in the stools were scored daily, and these scores were summed to calculate the Disease activity index (DAI). These parameters were scored according to a scale adapted from Cooper *et al* [64] and Hoffman *et al* [65] (Table 1).

**Macroscopic and microscopic evaluation of intestinal lesions:** The macroscopic features of intestinal lesions, *i.e.*, the presence of hyperemia and ulcers and the severity of intestinal inflammation, were scored according to the scale proposed by Wallace *et al* [66]. The microscopic features of the intestinal lesions, *i.e.*, the presence of ulcers, the severity of edema in the submucosal layer, and the degree of inflammatory cell infiltration, were scored according to the scale proposal by Fabia *et al* [67] following hematoxylin and eosin staining (Table 2).

**Table 1** Changes in weight, stool consistency, and the presence of blood in the stool were scored for the ulcerative colitis model mice and mice that received intrarectal injection of 35% ethanol according to the following scale

Disease activity index		Score
A	Weight change (< 1%)	0
	Weight change (1%-2%)	1
	Weight change (2%-4%)	2
	Weight change (4%-6%)	3
	Weight change (> 6%)	4
B	Stool consistency (normal)	0
	Stool consistency (normal and well-formed)	1
	Stool consistency (pasty that did not stick to the anus)	2
	Stool consistency (loose stool)	3
	Stool consistency (diarrhea)	4
C	Rectal bleeding (absent)	0
	Rectal bleeding (+)	1
	Rectal bleeding (++)	2
	Rectal bleeding (+++)	3
	Rectal bleeding (gross bleeding)	4

A: Weight; B: Stool consistency; C: Presence of blood in the stool.

### Immunohistochemistry

The large intestines of all mice were washed in PBS, stretched, fixed with the mucosa facing down on wooden platforms, and submerged in 4% paraformaldehyde in 0.1 M PBS (pH 7.3) for 24 h at 4 °C. Subsequently, the tissues were bleached by three 10-min washes in 100% dimethyl sulfoxide (Synth, Brazil) and then washed three more 10-min washes in PBS for 10 min each. Finally, the samples were stored at 4 °C in PBS containing sodium azide (0.1%).

To prepare whole mounts, the mucosal and submucosal layers and the circular muscle layer were removed from segments of the distal colon, leaving only the longitudinal muscle layer and the myenteric plexus. The whole mounts were preincubated for 45 min at room temperature with 10% normal horse serum in PBS containing 1.5% Triton X-100. The tissues were incubated for 48 h at 4 °C with the primary antibodies (Table 3). After 48 h of primary antibody incubation, the preparations were washed three times in PBS for 10 min each and then incubated for one hour at room temperature with the secondary antibodies (Table 3). Finally, they were washed three times for 10 min each in PBS, incubated in 4',6'-diamino-2-phenyl-indol (DAPI) for three minutes, and washed three times in PBS for five minutes each. Whole mounts were mounted on slides in glycerol buffered with 0.5 M sodium carbonate (pH 8.6).

Qualitative analysis of the myenteric neurons was performed on a Nikon 80i fluorescence microscope and an Olympus FluoView 1000 confocal laser microscope. The captured images were processed with CorelDRAW software.

### Quantitative analyses

The neuronal density (number of neurons per ganglion) was obtained by counting calretinin-immunoreactive (ir) and P2X7 receptor-ir neurons in 50 myenteric ganglia of the distal colon of each animal at 40 × magnification under a Nikon 80i microscope. The slides were analyzed in a zigzag pattern, and the ganglia were chosen randomly. In total, 2000 myenteric ganglia were analyzed for each protein of interest.

For analysis of the neuronal profile area, 125 calretinin-ir neurons in the distal colon myenteric plexus of each animal were randomly photographed at 40 × magnification under a Nikon 80i microscope *via* NIS-elements AR 3.1 software. For analysis of the nuclear profile area, the DAPI-labeled nuclei of these same 125 neurons were photographed. Neuronal and nuclear morphometry was performed by manually delimiting each of the structures individually in Image Pro-Plus 5.0 software. The cytoplasmic profile area was obtained by subtracting the nuclear area from the neuronal area. The results are presented in  $\mu\text{m}^2$ . In total, 5000 neurons and 5000 nuclei were analyzed.

**Table 2** Scale used to score the severity of macroscopic and microscopic lesions in the distal colon of ulcerative colitis model mice and mice that received intrarectal injection of 35% ethanol

Macroscopic injury	Score
Normal	0
Hyperemia without ulcers	1
Ulcerations without hyperemia	2
Ulcerations at one site	3
Ulcerations at two or more sites	4
Sites of damage extending > 1 cm	5
Sites of damage extending > 2 cm; the score increases by 1 for each additional cm	6-10
<b>A</b>	
No ulcer	0
Single ulceration not exceeding the lamina muscularis mucosa	1
Ulcerations not exceeding the mucosa	2
Ulcerations exceeding the submucosa	3
<b>B</b>	
No submucosal edema	0
Mild edema	1
Moderate edema	2
Severe edema	3
<b>C</b>	
No inflammatory cell infiltration	0
Mild infiltration	1
Moderate infiltration	2
Dense infiltration	3

The presence of ulcers (A), the severity of edema in the submucosal layer (B), and the degree of inflammatory cell infiltration (C) were assessed by histological analysis.

**Table 3** Characteristics of primary and secondary antibodies

Antigen	Host	Dilution	Source
Calretinin	Goat	1:300	Swant
P2X7 receptor	Rabbit	1:200	Merck Millipore
Cleaved caspase-3	Rabbit	1:100	Cell Signaling
Total caspase-3	Rabbit	1:100	Cell Signaling
Phospho- NF-κB	Rabbit	1:100	Cell Signaling
Total NF-κB (p65)	Rabbit	1:100	Cell Signaling
Secondary antibodies			
Alexa Fluor 488-conjugated donkey anti-rabbit IgG	Donkey	1:500	Molecular Probes
Alexa Fluor 594-conjugated donkey anti-sheep IgG	Donkey	1:100	Molecular Probes

NF-κB: Nuclear factor kappa B.

For corrected total cell fluorescence (CTCF) analysis, 20 calretinin-ir, P2X7 receptor-ir, cleaved caspase-3-ir, total caspase-3-ir, phospho- NF- $\kappa$ B-ir, and total NF- $\kappa$ B-ir ganglia of the myenteric plexus of the distal colon of each animal were photographed at 40  $\times$  magnification under a Nikon 80i microscope *via* NIS-elements AR 3.1 software. The ganglia were individually delineated in ImageJ software (v1.45, NIH). The area, integrated density, and average gray value of each ganglion were systematically measured. The areas, integrated densities, and average gray values of five regions adjacent to the myenteric ganglion that were not positive for the protein of interest were measured as background values. The CTCF was calculated by the following formula: CTCF = integrated density - (area of the selected ganglion  $\times$  average background fluorescence)[68,69]. In total, 800 myenteric ganglia were analyzed for each protein of interest.

### Transmission electron microscopy

An approximately 0.5 cm piece of the distal colon of each mouse was collected for ultrastructural analysis of the myenteric plexus by transmission electron microscopy. Immediately after collection, the samples were cut into three-millimeter pieces. The samples were fixed for three hours at 4  $^{\circ}$ C in modified Karnovsky solution (4.0% formaldehyde, 0.2 M phosphate buffer and 25% glutaraldehyde) and postfixed for two hours at 4  $^{\circ}$ C in 1% osmium tetroxide. Then, the tissues were placed in 0.5% uranyl acetate for 12 h at room temperature, dehydrated by sequential incubations in alcohol solutions of increasing concentrations, and immersed in propylene oxide twice for 15 min each. Finally, the tissues were incubated in a 1:1 mixture of Spurr resin and propylene oxide for one hour, a 3:1 mixture of Spurr resin and propylene oxide for one and a half hours, and pure resin for 12 h. The tissues were then embedded in pure Spurr resin for three days in an oven at 60  $^{\circ}$ C. Semifine 250 nanometer (nm)-thick semithin sections were made with a Leica Ultracut UCT ultramicrotome, and the sections were stained with 1% toluidine blue for one and a half minutes and then washed with distilled water. Then, the sections were cut into 60 nm thick ultrathin sections, collected on 200 mesh copper screens and contrasted with uranyl acetate for five minutes and lead citrate 1% for three minutes. The prepared screens were analyzed with a Morgagni 268D transmission electron microscope, and the captured images were processed with CorelDRAW software.

### Tissue preparation and histological analysis

An approximately 0.5 cm piece of the distal colon of each mouse was collected for histological analysis. After being washed in PBS, the samples were fixed with the mucosa facing up on wooden platforms and immersed in 4% paraformaldehyde in 0.1 M PBS (pH 7.3) for 48 h at 4  $^{\circ}$ C. Then, the tissues were dehydrated by sequential incubation in alcohol solutions of increasing concentrations, diaphanized in xylol, and embedded in paraffin. The samples were cut into five  $\mu$ m thick transverse sections with a specialized microtome and subjected to hematoxylin and eosin staining. Picrosirius red and Masson's trichrome were used to visualize collagen fibers, and periodic acid-Schiff staining was used to identify neutral mucin-secreting goblet cells. The slides were analyzed under light and polarized light microscopy with a Nikon 80i microscope. Images were captured *via* NIS-elements AR 3.1 software and processed with CorelDRAW software.

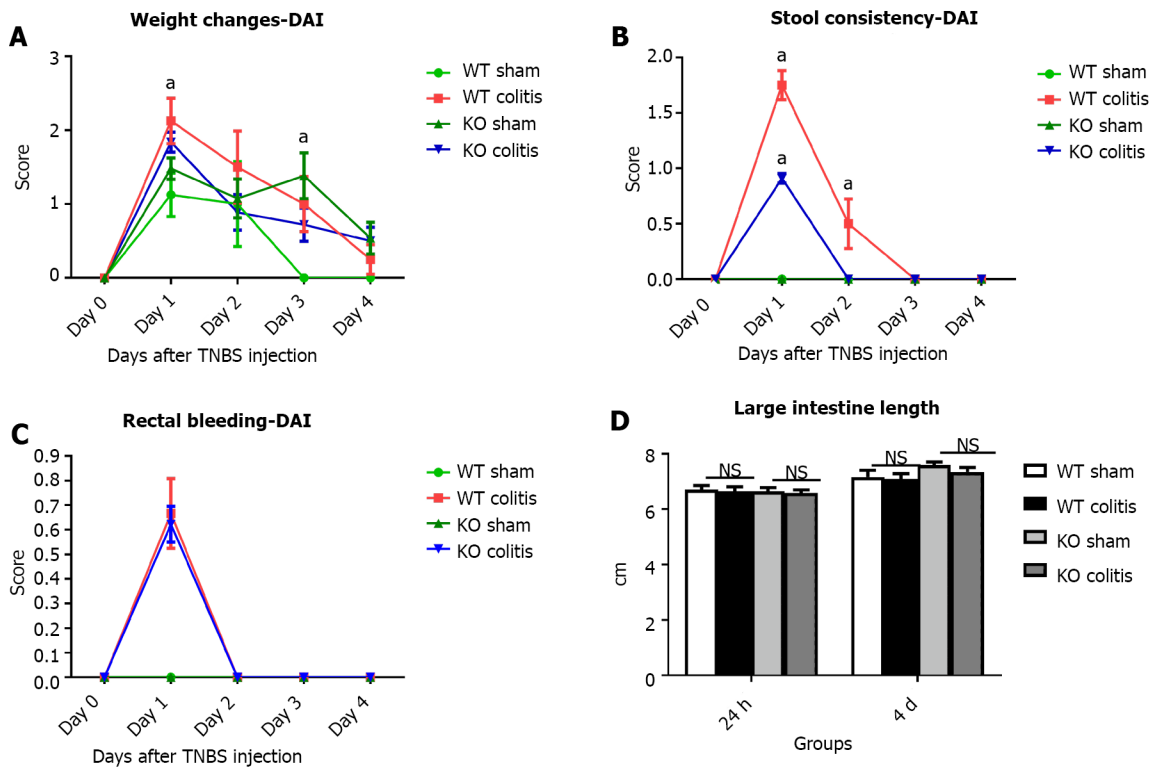
**Analysis of the number of goblet cells per intestinal crypt of the distal colon:** The density of goblet cells (number of goblet cells per intestinal crypt) was determined by counting goblet cells in 40 intestinal crypts of the distal colon *via* periodic acid Schiff staining. Four histological sections per animal were analyzed with a Nikon 80i microscope with a 40  $\times$  objective[70-73]. Sections separated by an interval of 10  $\mu$ m were analyzed, and crypts were chosen randomly. In total, 1600 crypts of the distal colon were analyzed.

### Statistical analysis

Quantitative data were analyzed, and the results are expressed as the mean  $\pm$  SE. Comparisons between groups were performed by two-way ANOVA followed by Bonferroni correction with GraphPad Prism 5.0 software. Statistical significance is displayed as  $P < 0.05$ .

## RESULTS

At 24 h, the average reduction in weight was 1.5% in the WT sham group, 3.5% in the WT colitis group, 2.4% in the KO sham group, and 2.7% in the KO colitis group. By four days, the animals in all groups recovered weight. Regarding the DAI, scores for weight change, stool consistency, and the presence of blood in stool were higher in the WT colitis group than in the WT sham group and in the KO colitis group than in the KO sham group. There was no statistically significant difference in large intestine length between the WT colitis (24 h and 4 d) and WT sham (24 h and 4 d) groups or between the KO colitis (24 h and 4 d) and KO sham (24 h and 4 d) groups (Figure 1). According to macroscopic analysis, tissue hyperemia without ulcers was observed in the 24 h and 4 d WT colitis and 24 h KO colitis groups. Microscopic analysis was performed after hematoxylin and eosin staining. No ulceration was observed



DOI: 10.3748/wjg.v29.i22.3440 Copyright ©The Author(s) 2023.

**Figure 1** The disease activity index of wild-type and knockout mice was determined beginning the day of ulcerative colitis induction or intrarectal injection of 35% ethanol. A: Changes in weight; B: Stool consistency; C: The presence of blood in the stool; D: Large intestine length was analyzed. DAI: Disease activity index; WT: Wild-type; KO: Knockout; TNBS: 2,4,6-trinitrobenzene sulfonic acid. The data are presented as the arithmetic mean  $\pm$  SE. <sup>a</sup> $P < 0.05$  vs sham groups; NS: Not significant.

in the analyzed tissues. Edema of the submucosal layer was observed in all groups, but with the mean score, edema was higher in the WT colitis 24 h group. Finally, inflammatory cell infiltration in the mucosa and lamina propria was severe in the WT colitis 24 h group but was mild in the other groups (Table 4).

### Qualitative analysis

Indirect immunofluorescence analysis revealed that neurons in the myenteric plexus of the distal colon were positive for calretinin, P2X7 receptor, cleaved caspase-3, total caspase-3, phospho-NF- $\kappa$ B, and total NF- $\kappa$ B.

Calretinin-ir neurons showed a Dogiel type II morphology, and calretinin was localized in the nucleus and cytoplasm. In the WT colitis 24 h and 4 d groups, there was an apparent reduction in fluorescence intensity, and in the WT colitis 24 h and KO colitis 24 h groups, the neurons appeared swollen. There was also an apparent reduction in the number of neurons in the WT colitis 24 h and 4 d and KO colitis 24 h groups (Figures 2-6).

The P2X7 receptor was expressed in the plasma membrane and cytoplasm. The P2X7 receptor staining intensity appeared to be stronger in the WT colitis 24 h group and weaker in the WT colitis 4 d group. There was an apparent reduction in the number of P2X7 receptor-ir cells in both groups, and the P2X7 receptor-ir cells colocalized with calretinin-ir neurons. P2X7 receptor staining was not observed in the KO sham 24 h, KO sham 4 d, KO colitis 24 h or KO colitis 4 d groups (Figure 2).

Cleaved caspase-3 was localized in the cytoplasm, and the cleaved caspase-3 fluorescence intensity was apparently higher in the WT colitis 24 h and 4 d groups and KO colitis 24 h group. Cleaved caspase-3 colocalized with calretinin-ir neurons in all groups, especially the colitis groups (WT colitis 24 h and 4 d and KO colitis 24 h and 4 d groups) (Figure 3). Total caspase-3, on the other hand, was expressed in the nucleus and cytoplasm, and the total caspase-3 fluorescence intensity was apparently similar among all groups. Total caspase-3 colocalized with calretinin-ir neurons, and nuclear staining of total caspase-3 was the lowest in the WT colitis 24 h group (Figure 4).

Phospho-NF- $\kappa$ B and total NF- $\kappa$ B were expressed in the cytoplasm. Phospho-NF- $\kappa$ B staining appeared to be more intense in the WT colitis 24 h group (Figure 5). Phospho-NF- $\kappa$ B and total NF- $\kappa$ B colocalized with calretinin-ir neurons in all groups (Figure 6).

**Table 4 Macroscopic and microscopic lesions in the distal colon of ulcerative colitis model mice and mice that received intrarectal injection of 35% ethanol**

Groups	Macroscopic injury	Microscopic injury		
		Ulcer	Submucosal edema	Inflammatory cell infiltration
WT sham 24 h	0.0 ± 0.0 <sup>NS</sup>	0.0 ± 0.0 <sup>NS</sup>	0.8 ± 0.2 <sup>NS</sup>	1.2 ± 0.2 <sup>NS</sup>
WT colitis 24 h	1.0 ± 0.0 <sup>NS</sup>	0.0 ± 0.0 <sup>NS</sup>	1.6 ± 0.2 <sup>NS</sup>	2.0 ± 0.2 <sup>NS</sup>
KO sham 24 h	0.0 ± 0.0 <sup>NS</sup>	0.0 ± 0.0 <sup>NS</sup>	0.8 ± 0.2 <sup>NS</sup>	1.0 ± 0.0 <sup>NS</sup>
KO colitis 24 h	0.4 ± 0.1 <sup>NS</sup>	0.0 ± 0.0 <sup>NS</sup>	0.8 ± 0.4 <sup>NS</sup>	1.2 ± 0.2 <sup>NS</sup>
WT sham 4 d	0.0 ± 0.0 <sup>NS</sup>	0.0 ± 0.0 <sup>NS</sup>	1.0 ± 0.2 <sup>NS</sup>	1.0 ± 0.0 <sup>NS</sup>
WT colitis 4 d	0.5 ± 0.2 <sup>NS</sup>	0.0 ± 0.0 <sup>NS</sup>	1.0 ± 0.0 <sup>NS</sup>	1.2 ± 0.2 <sup>NS</sup>
KO sham 4 d	0.0 ± 0.0 <sup>NS</sup>	0.0 ± 0.0 <sup>NS</sup>	0.6 ± 0.2 <sup>NS</sup>	0.4 ± 0.2 <sup>NS</sup>
KO colitis 4 d	0.0 ± 0.0 <sup>NS</sup>	0.0 ± 0.0 <sup>NS</sup>	0.8 ± 0.2 <sup>NS</sup>	0.4 ± 0.2 <sup>NS</sup>

The presence of ulcers, severity of edema in the submucosal layer, and degree of inflammatory cell infiltration were assessed by histological analysis. NS: Not significant; WT: Wild-type; KO: Knockout.

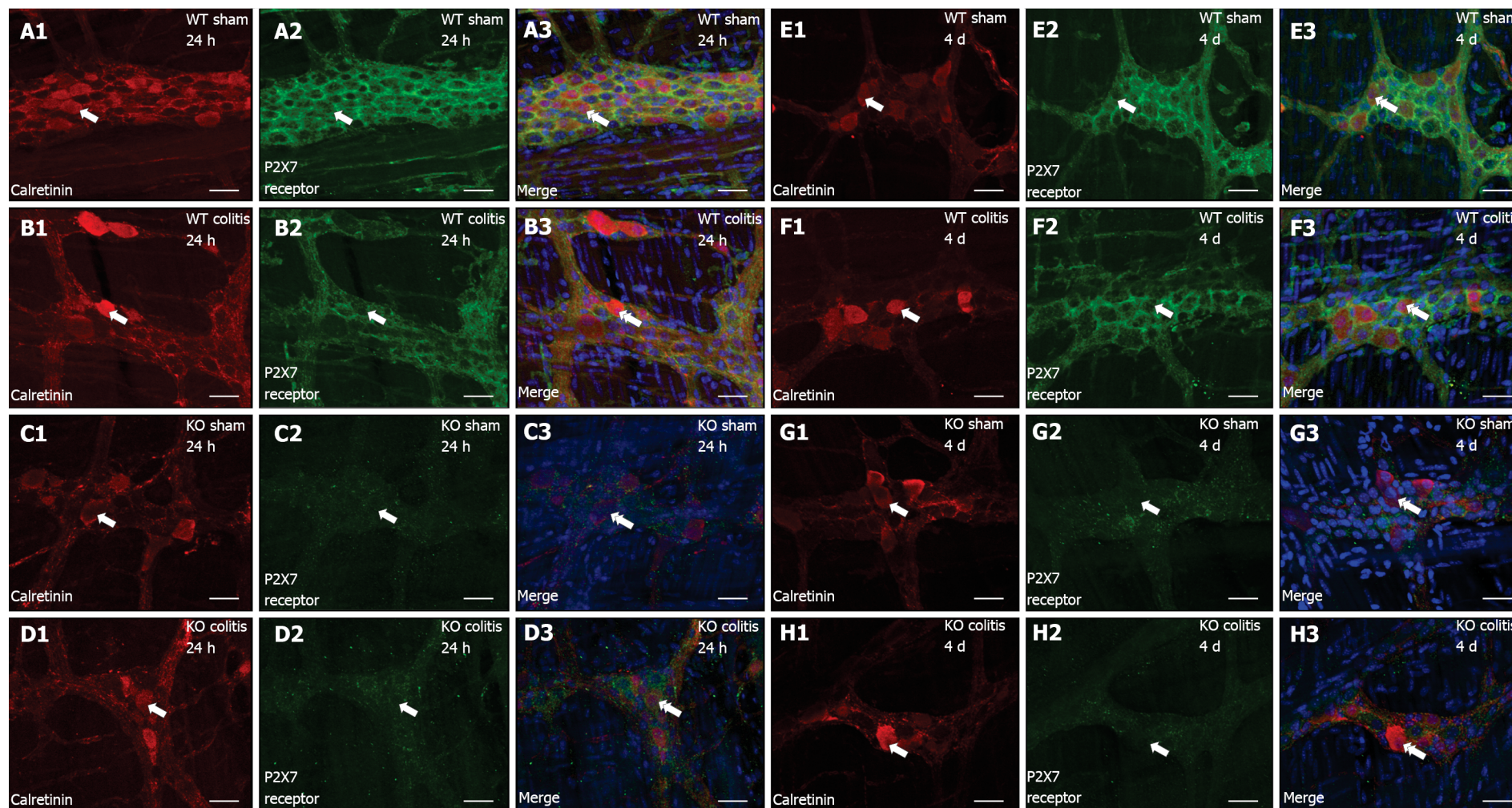
### Quantitative analyses

The number of calretinin-ir neurons per myenteric ganglion of the distal colon was decreased by 36.9% in the WT colitis 24 h group compared to the WT sham 24 h group ( $2.1 \pm 0.13$  vs  $3.33 \pm 0.17$ ,  $P < 0.001$ ) and decreased by 21.1% in the WT colitis 4 d group compared to the WT sham 4 d group ( $2.92 \pm 0.12$  vs  $3.7 \pm 0.11$ ,  $P < 0.05$ ). No statistically significant differences in calretinin-ir neuron density were observed between the KO colitis (24 h and 4 d) groups and the KO sham (24 h and 4 d) groups (Figure 7A).

The number of P2X7-ir receptor neurons per myenteric ganglion of the distal colon was decreased by 12.2% in the WT colitis 24 h group compared to the WT sham 24 h group ( $19.49 \pm 0.35$  vs  $22.21 \pm 0.18$ ,  $P < 0.001$ ) and decreased by 10.5% in the WT colitis 4 d group compared to the WT sham 4 d group ( $20.35 \pm 0.14$  vs  $22.75 \pm 0.51$ ,  $P < 0.001$ ). No P2X7 receptor-ir neurons were observed in the myenteric ganglia in the KO sham (24 h and 4 d) or KO colitis (24 h and 4 d) groups (Figure 7B).

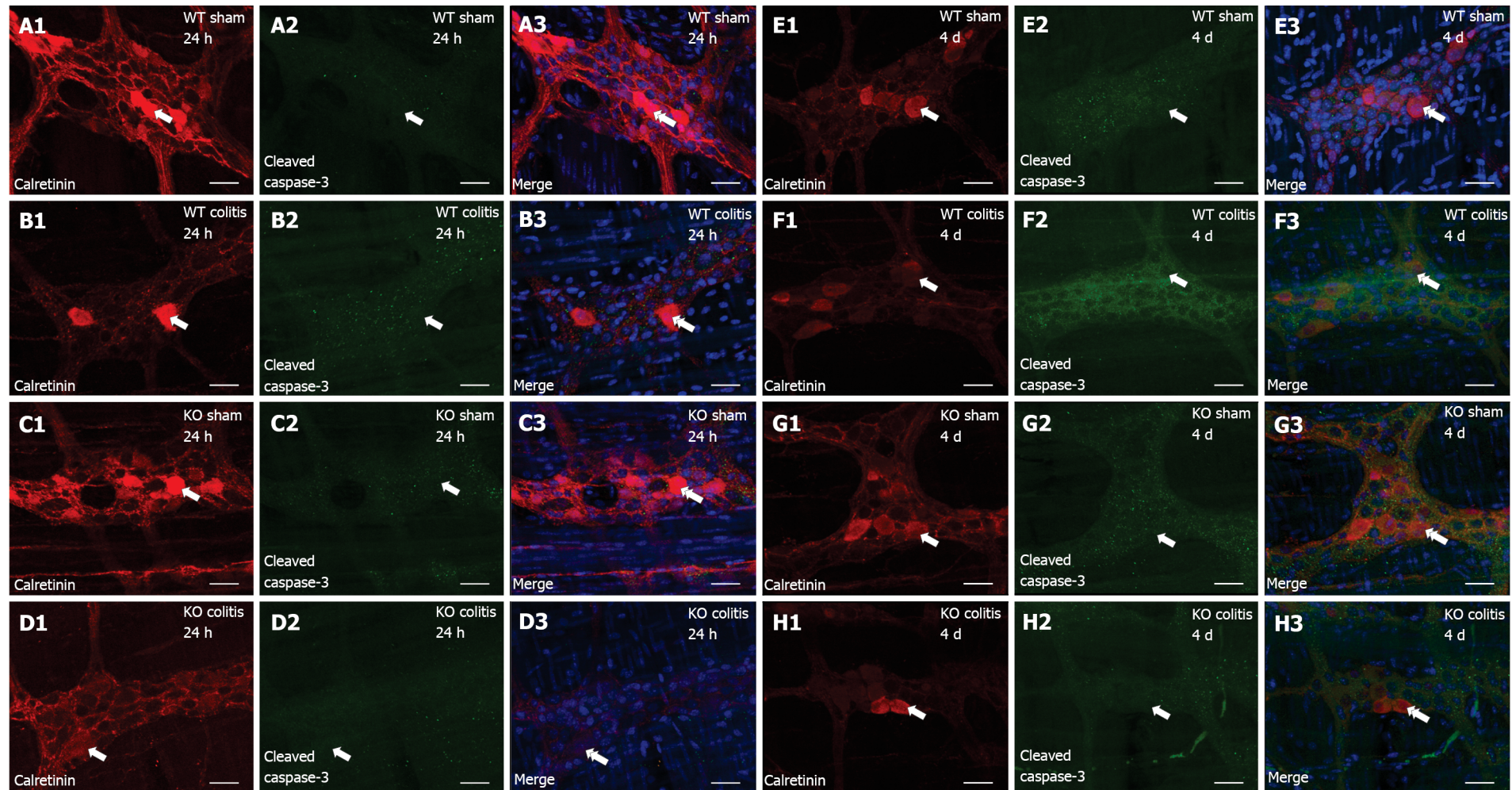
The profile area of calretinin-ir neurons in the myenteric plexus of the distal colon was increased by 10.9% in the WT colitis 24 h group compared to the WT sham 24 h group ( $312.6 \pm 7.85$  vs  $278.41 \pm 6.65$ ,  $P < 0.05$ ) and increased by 14.6% in the KO colitis 24 h group compared to the KO sham 24 h group ( $302.99 \pm 16.78$  vs  $258.67 \pm 9.49$ ,  $P < 0.01$ ). The neuronal profile area was decreased by 16.4% in the WT colitis 4 d group compared to the WT sham 4 d group ( $277.23 \pm 9.94$  vs  $331.54 \pm 7.63$ ,  $P < 0.001$ ), and there was no difference in this measure between the KO colitis 4 d and KO sham 4 d groups (Figure 8A). The nuclear profile area in the WT colitis 4 d group was decreased by 10.9% compared to that in the WT sham 4 d group ( $104.63 \pm 2.49$  vs  $117.41 \pm 1.14$ ,  $P < 0.01$ ). No statistically significant differences in nuclear profile area were observed between the KO colitis (24 h and 4 d) groups and the KO sham (24 h and 4 d) groups (Figure 8B). The cytoplasmic profile area of calretinin-ir neurons in the myenteric plexus of the distal colon was increased by 15% in the WT colitis 24 h group compared to the WT sham 24 h group ( $195.86 \pm 6.88$  vs  $166.37 \pm 5.98$ ,  $P < 0.05$ ) and increased by 20.4% in the KO colitis 24 h group compared to the KO sham 24 h group ( $178.88 \pm 15.52$  vs  $142.41 \pm 8.62$ ,  $P < 0.05$ ). The cytoplasmic profile area in the WT colitis 4 d group was decreased by 19.4% compared with that in the WT sham 4 d group ( $172.61 \pm 10.4$  vs  $214.13 \pm 6.73$ ,  $P < 0.01$ ). No statistically significant difference in the cytoplasmic profile area was observed between the KO colitis 4 d group and the KO sham 4 d group (Figure 8C).

The profile area of calretinin-ir neurons in the myenteric plexus of the distal colon ranged from 50  $\mu\text{m}^2$  to 1050  $\mu\text{m}^2$ . In the WT sham 24 h, WT colitis 24 h and KO colitis 24 h groups, 54.4%, 48.0%, and 59.5% of calretinin-ir neurons, respectively, had an area between 200  $\mu\text{m}^2$  and 300  $\mu\text{m}^2$ . In the KO sham 24 h group, 58.5% of neurons had an area between 100  $\mu\text{m}^2$  and 200  $\mu\text{m}^2$  (Figure 9A). In the WT sham 4 d, WT colitis 4 d, KO sham 4 d and KO colitis 4 d groups, 58.1%, 65.6%, 62.7% and 60.6% of calretinin-ir neurons, respectively, had an area between 200  $\mu\text{m}^2$  and 300  $\mu\text{m}^2$  (Figure 9B). The nuclear profile area of these same calretinin-ir neurons ranged from 50  $\mu\text{m}^2$  to 230  $\mu\text{m}^2$ . In the WT sham 24 h and KO sham 24 h groups, 57.9% and 52.6% of calretinin-ir neurons, respectively, had a nuclear area between 90  $\mu\text{m}^2$  and 110  $\mu\text{m}^2$ . In the WT colitis 24 h and KO colitis 24 h groups, 62.4% and 55.5% of calretinin-ir neurons, respectively, had a nuclear area between 110  $\mu\text{m}^2$  and 130  $\mu\text{m}^2$  (Figure 9C). In the WT colitis 4 d group, 63.5% of calretinin-ir neurons had a nuclear area between 90  $\mu\text{m}^2$  and 110  $\mu\text{m}^2$ , and in the WT sham 4 d, KO sham 4 d and KO colitis 4 d groups, 62.4%, 52.6% and 55% of calretinin-ir neurons, respectively, had a nuclear area between 110  $\mu\text{m}^2$  and 130  $\mu\text{m}^2$  (Figure 9D). Finally, the cytoplasmic profile area of these same calretinin-ir neurons ranged from 0  $\mu\text{m}^2$  to 840  $\mu\text{m}^2$ . In the WT sham 24 h and WT colitis 24 h groups, 55.3% and 50.2% of calretinin-ir neurons, respectively, had a cytoplasmic area between 130  $\mu\text{m}^2$



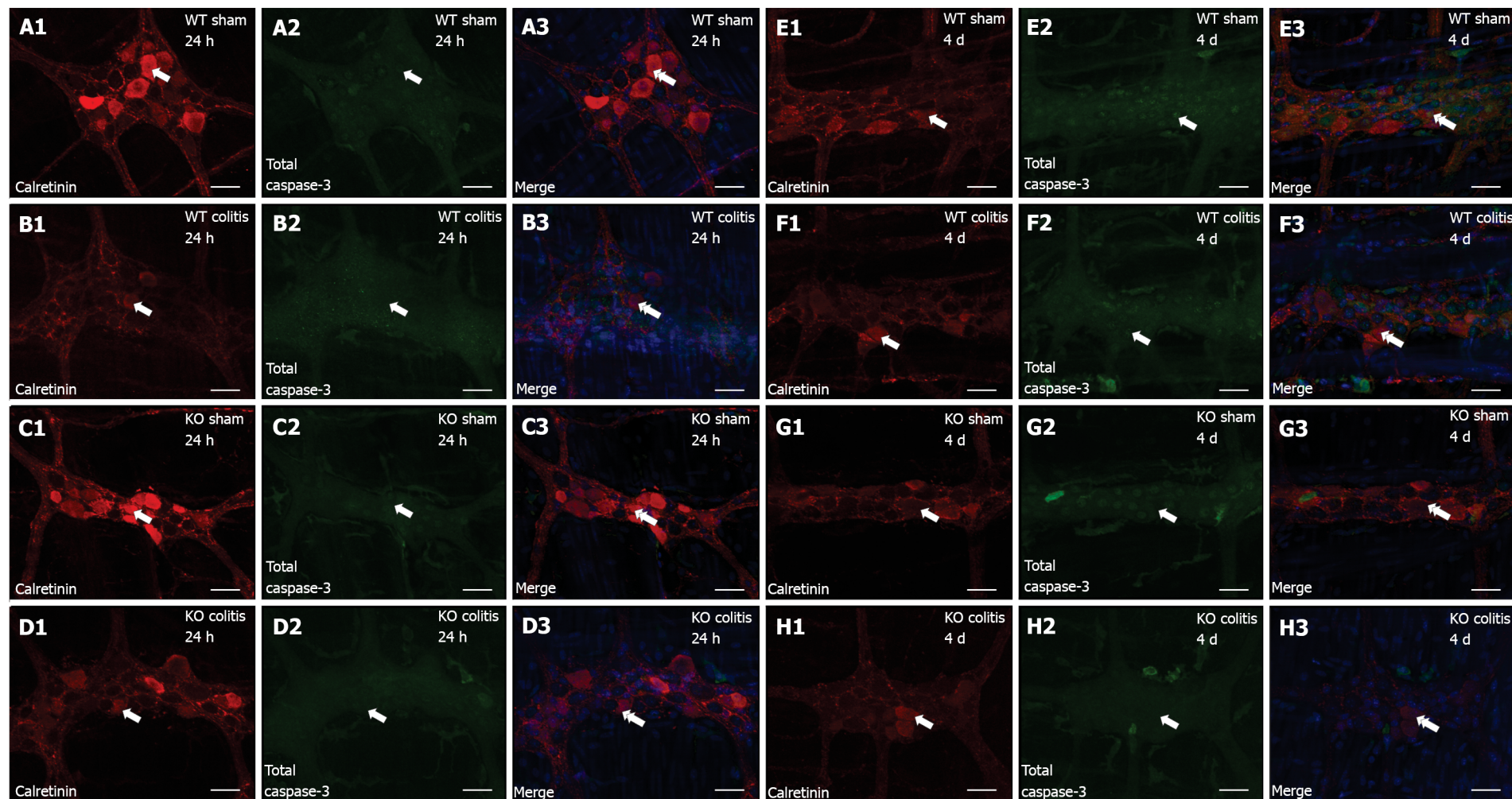
DOI: 10.3748/wjg.v29.i22.3440 Copyright ©The Author(s) 2023.

**Figure 2** Colocalization of calretinin (red) with the P2X7 receptor (green) and DAPI (blue) in neurons in the myenteric plexus of the distal colon in mice. A1-A3: Wild-type (WT) sham 24 h; B1-B3: WT colitis 24 h; C1-C3: Knockout (KO) sham 24 h; D1-D3: KO colitis 24 h; E1-E3: WT sham 4 d; F1-F3: WT colitis 4 d; G1-G3: KO sham 4 d; H1-H3: KO colitis 4 d groups. The single arrows indicate calretinin-ir (A1-H1) and P2X7 receptor-ir (A2-H2) neurons, and the double arrows indicate the colocalization of calretinin with the P2X7 receptor and DAPI (A3-H3). Scale bar = 30  $\mu$ m. WT: Wild-type; KO: Knockout.



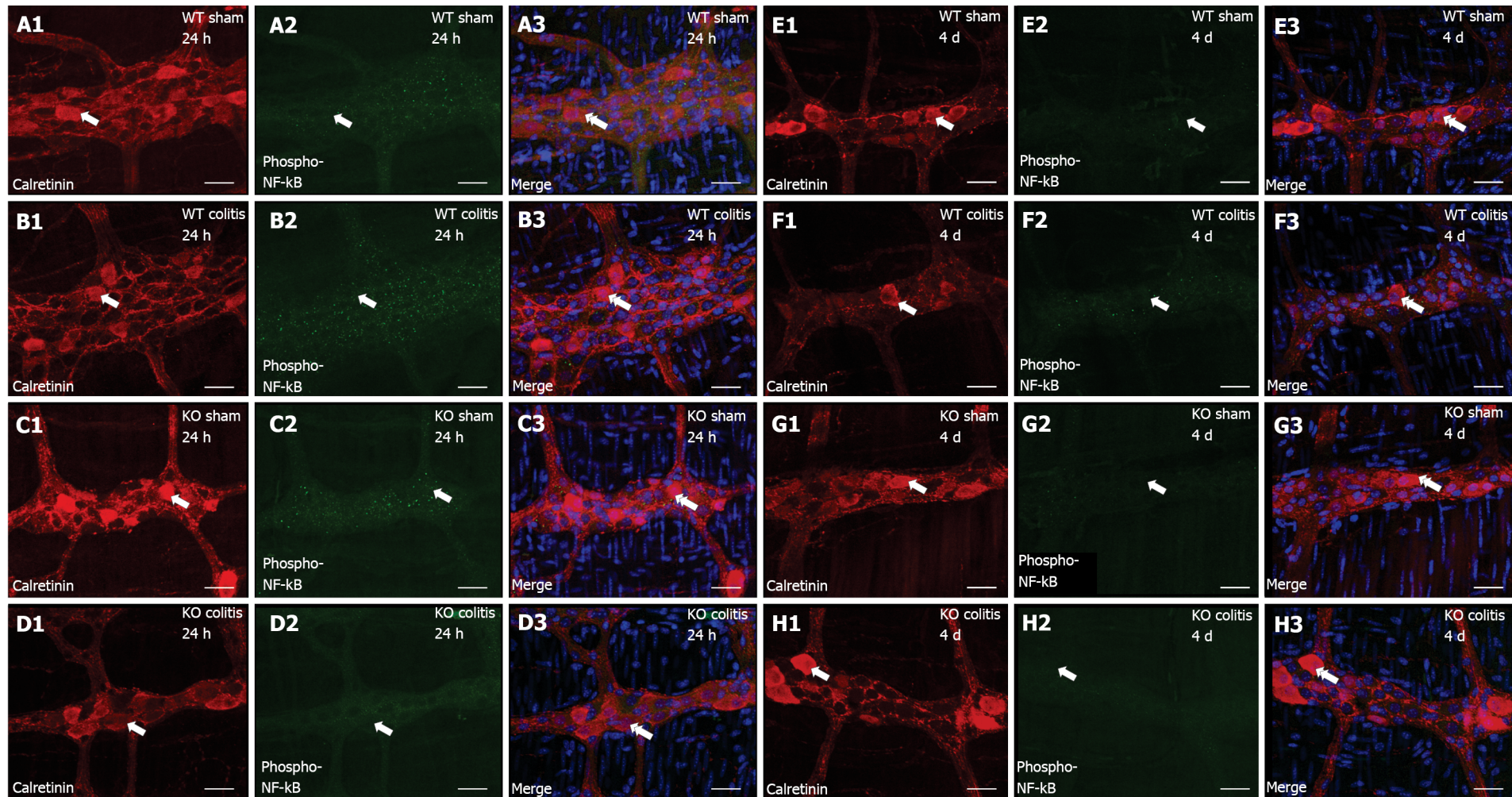
DOI: 10.3748/wjg.v29.i22.3440 Copyright ©The Author(s) 2023.

**Figure 3** Colocalization of calretinin (red) with cleaved caspase-3 (green) and DAPI (blue) in neurons in the myenteric plexus of the distal colon in mice of different groups. A1-A3: Wild-type (WT) sham 24 h; B1-B3: WT colitis 24 h; C1-C3: Knockout (KO) sham 24 h; D1-D3: KO colitis 24 h; E1-E3: WT sham 4 d; F1-F3: WT colitis 4 d; G1-G3: KO sham 4 d; and H1-H3: KO colitis 4 d groups. The single arrows indicate calretinin-ir (A1-H1) and cleaved caspase-3-ir (A2-H2) neurons, and the double arrows indicate the colocalization of calretinin with cleaved caspase-3 and DAPI (A3-H3). Scale bar = 30  $\mu$ m. WT: Wild-type; KO: Knockout.



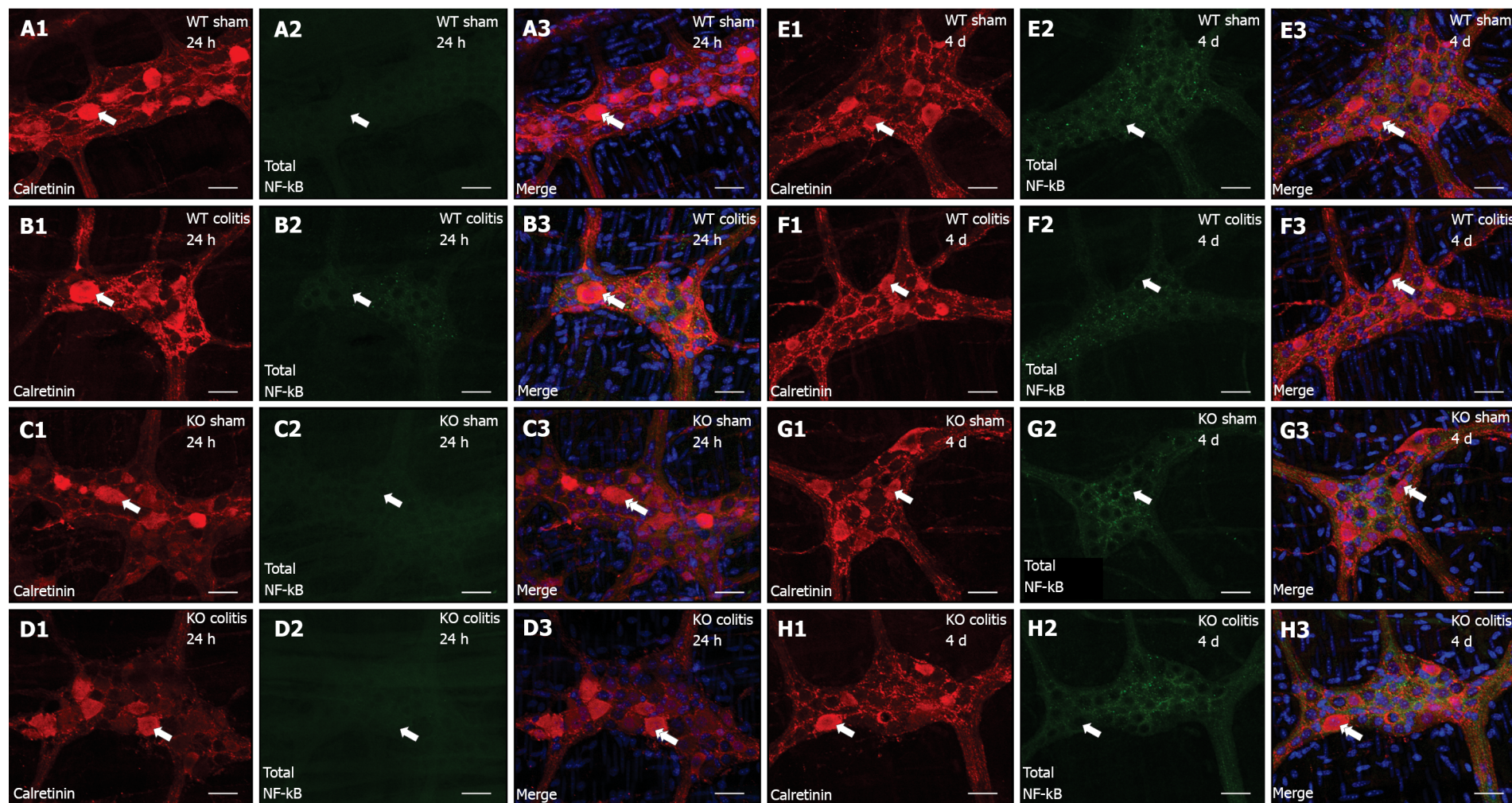
DOI: 10.3748/wjg.v29.i22.3440 Copyright ©The Author(s) 2023.

**Figure 4** Colocalization of calretinin (red) with total caspase-3 (green) and DAPI (blue) in neurons in the myenteric plexus of the distal colon in mice of different groups. A1-A3: Wild-type (WT) sham 24 h; B1-B3: WT colitis 24 h; C1-C3: Knockout (KO) sham 24 h; D1-D3: KO colitis 24 h; E1-E3: WT sham 4 d; F1-F3: WT colitis 4 d; G1-G3: KO sham 4 d; and H1-H3: KO colitis 4 d groups. The single arrows indicate calretinin-ir (A1-H1) and total caspase-3-ir (A2-H2) neurons, and the double arrows indicate the colocalization of calretinin with total caspase-3 and DAPI (A3-H3). Scale bar = 30  $\mu$ m. WT: Wild-type; KO: Knockout.



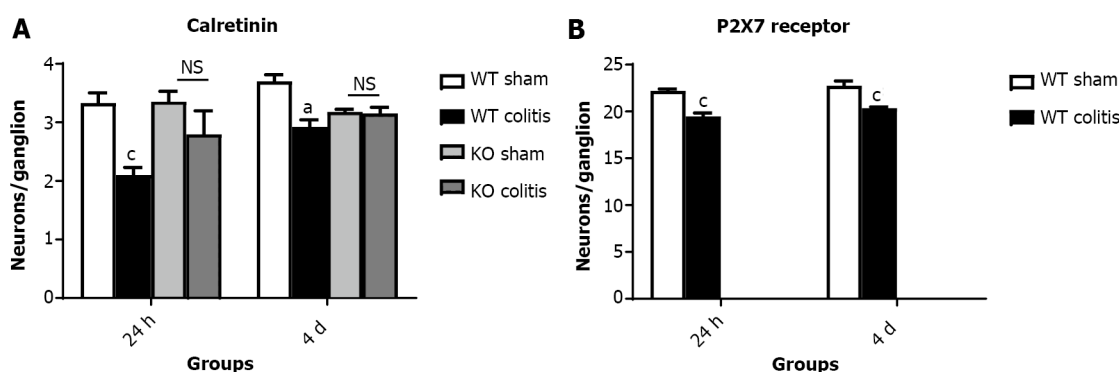
DOI: 10.3748/wjg.v29.i22.3440 Copyright ©The Author(s) 2023.

**Figure 5** Colocalization of calretinin (red) with phospho-nuclear factor kappa B (green) and DAPI (blue) in neurons in the myenteric plexus of the distal colon in mice of different groups. A1-A3: Wild-type (WT) sham 24 h; B1-B3: WT colitis 24 h; C1-C3: Knockout (KO) sham 24 h; D1-D3: KO colitis 24 h; E1-E3: WT sham 4 d; F1-F3: WT colitis 4 d; G1-G3: KO sham 4 d; and H1-H3: KO colitis 4 d groups. The single arrows indicate calretinin-ir (A1-H1) and phospho-nuclear factor kappa B (NF- $\kappa$ B)-ir (A2-H2) neurons, and the double arrows indicate the colocalization of calretinin with phospho- NF- $\kappa$ B and DAPI (A3-H3). Scale bar = 30  $\mu$ m. WT: Wild-type; KO: Knockout.



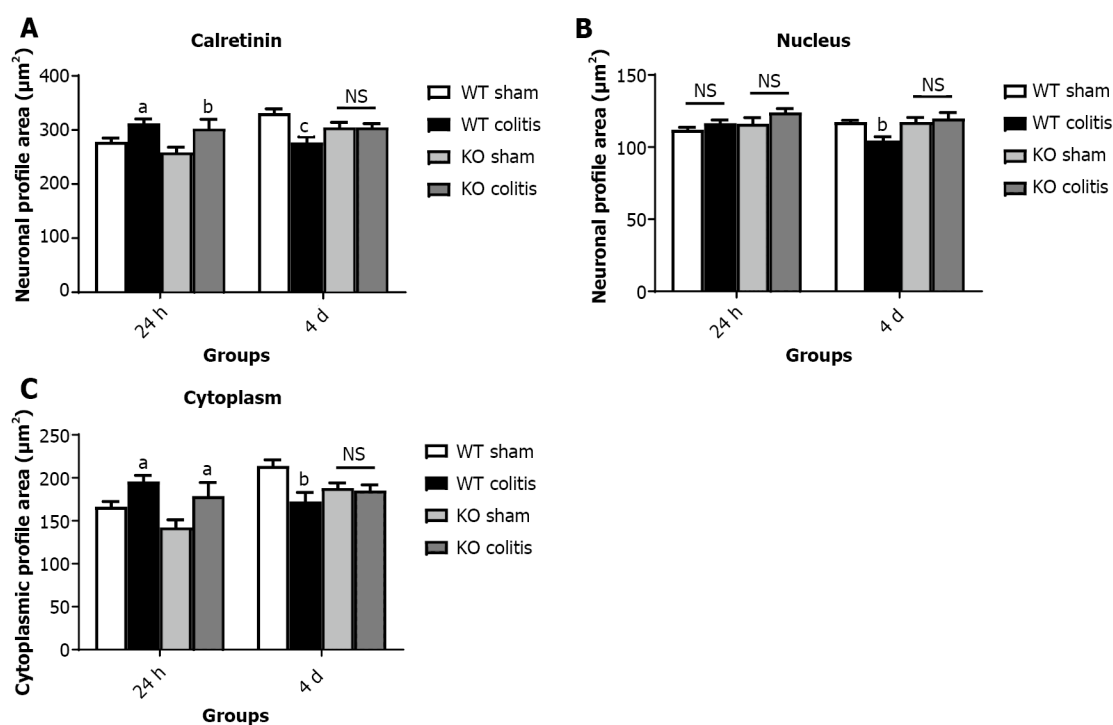
DOI: 10.3748/wjg.v29.i22.3440 Copyright ©The Author(s) 2023.

**Figure 6** Colocalization of calretinin (red) with total nuclear factor kappa B (green) and DAPI (blue) in neurons in the myenteric plexus of the distal colon in mice of different groups. A1-A3: Wild-type (WT) sham 24 h; B1-B3: WT colitis 24 h; C1-C3: Knockout (KO) sham 24 h; D1-D3: KO colitis 24 h; E1-E3: WT sham 4 d; F1-F3: WT colitis 4 d; G1-G3: KO sham 4 d; and H1-H3: KO colitis 4 d groups. The single arrows indicate calretinin-ir (A1-H1) and total nuclear factor kappa B (NF-κB)-ir (A2-H2) neurons, and the double arrows indicate the colocalization of calretinin with total NF-κB and DAPI (A3-H3). Scale bar = 30 μm. WT: Wild-type; KO: Knockout.



DOI: 10.3748/wjg.v29.i22.3440 Copyright ©The Author(s) 2023.

**Figure 7** Number of calretinin-ir and P2X7 receptor-ir neurons per myenteric ganglion in the distal colon in mice from the wild-type sham 24 h and 4 d, wild-type colitis 24 h and 4 d, knockout sham 24 h and 4 d, and knockout colitis 24 h and 4 d groups. A: Calretinin-ir; B: P2X7 receptor-ir. The data are presented as the arithmetic mean  $\pm$  SE. <sup>a</sup> $P < 0.05$  vs sham groups; <sup>c</sup> $P < 0.001$  vs sham groups; NS: Not significant. WT: Wild-type; KO: Knockout.

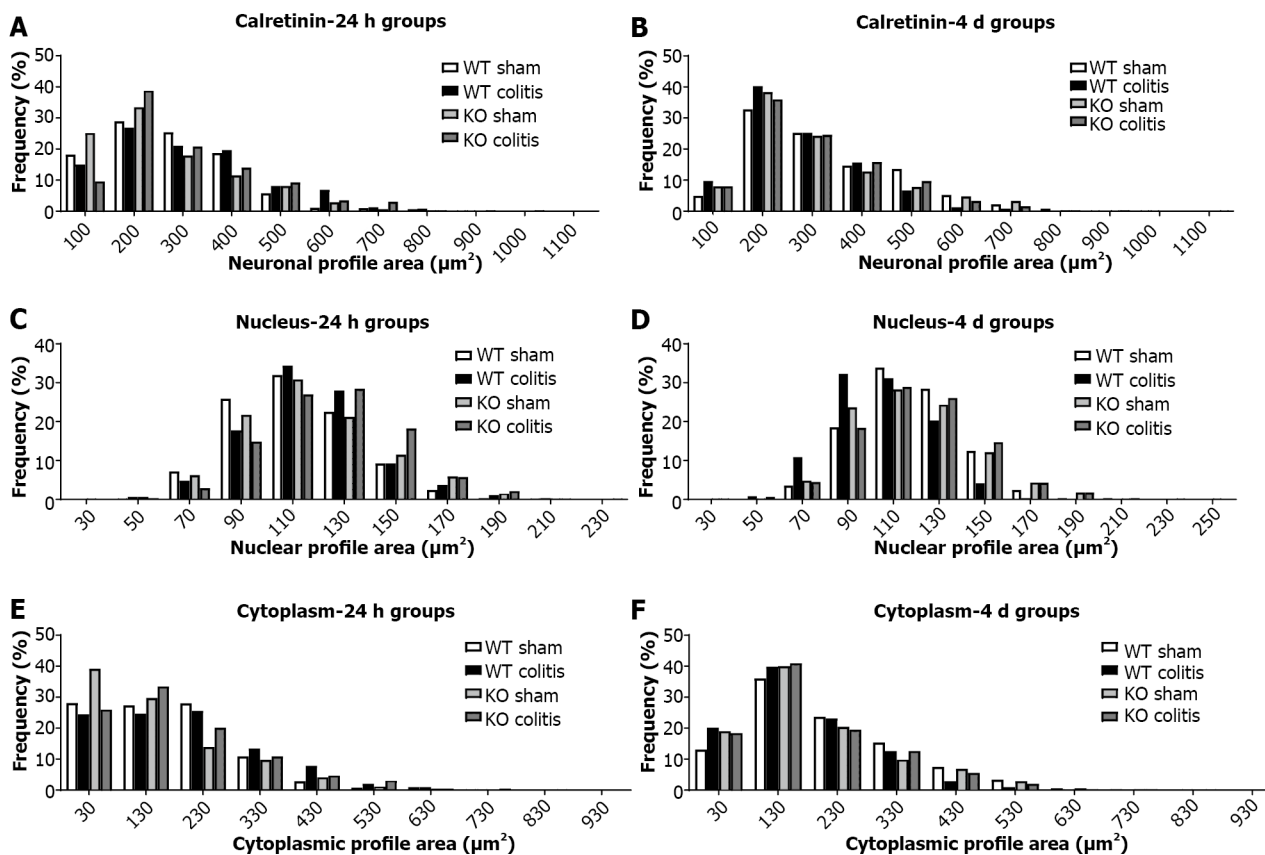


DOI: 10.3748/wjg.v29.i22.3440 Copyright ©The Author(s) 2023.

**Figure 8** Neuronal, nuclear, and cytoplasmic profile areas of calretinin-ir neurons in the myenteric plexus of the distal colon in mice from the wild-type sham 24 h and 4 d, wild-type colitis 24 h and 4 d, knockout sham 24 h and 4 d, and knockout colitis 24 h and 4 d groups. A: Neuronal; B: Nuclear; C: Cytoplasmic. The data are presented as the arithmetic mean  $\pm$  SE. <sup>a</sup> $P < 0.05$  vs sham groups; <sup>b</sup> $P < 0.01$  vs sham groups; <sup>c</sup> $P < 0.001$  vs sham groups; NS: Not significant. WT: Wild-type; KO: Knockout.

and 230  $\mu\text{m}^2$ . In the KO sham 24 h and KO colitis 24 h groups, 69% and 59.3% of calretinin-ir neurons, respectively, had a cytoplasmic area between 30  $\mu\text{m}^2$  and 130  $\mu\text{m}^2$  (Figure 9E). In the WT sham 4 d, WT colitis 4 d, KO sham 4 d and KO colitis 4 d groups, 59.7%, 63%, 60.5% and 60.5% of calretinin-ir neurons, respectively, had a cytoplasmic area between 130  $\mu\text{m}^2$  and 230  $\mu\text{m}^2$  (Figure 9F).

The CTCF of calretinin-ir ganglia in the myenteric plexus of the distal colon was decreased by 24.5% in the WT colitis 24 h group compared to the WT sham 24 h group ( $2322102 \pm 154255$  vs  $3076921 \pm 104235$ ,  $P < 0.001$ ) and was decreased by 13.7% in the WT colitis 4 d group compared to the WT sham 4 d group ( $2976603 \pm 52989$  vs  $3452123 \pm 30894$ ,  $P < 0.01$ ). No statistically significant differences in the CTCF of calretinin-ir myenteric ganglia were observed between the KO colitis (24 h and 4 d) groups and the KO sham (24 h and 4 d) groups (Figure 10A).



DOI: 10.3748/wjg.v29.i22.3440 Copyright ©The Author(s) 2023.

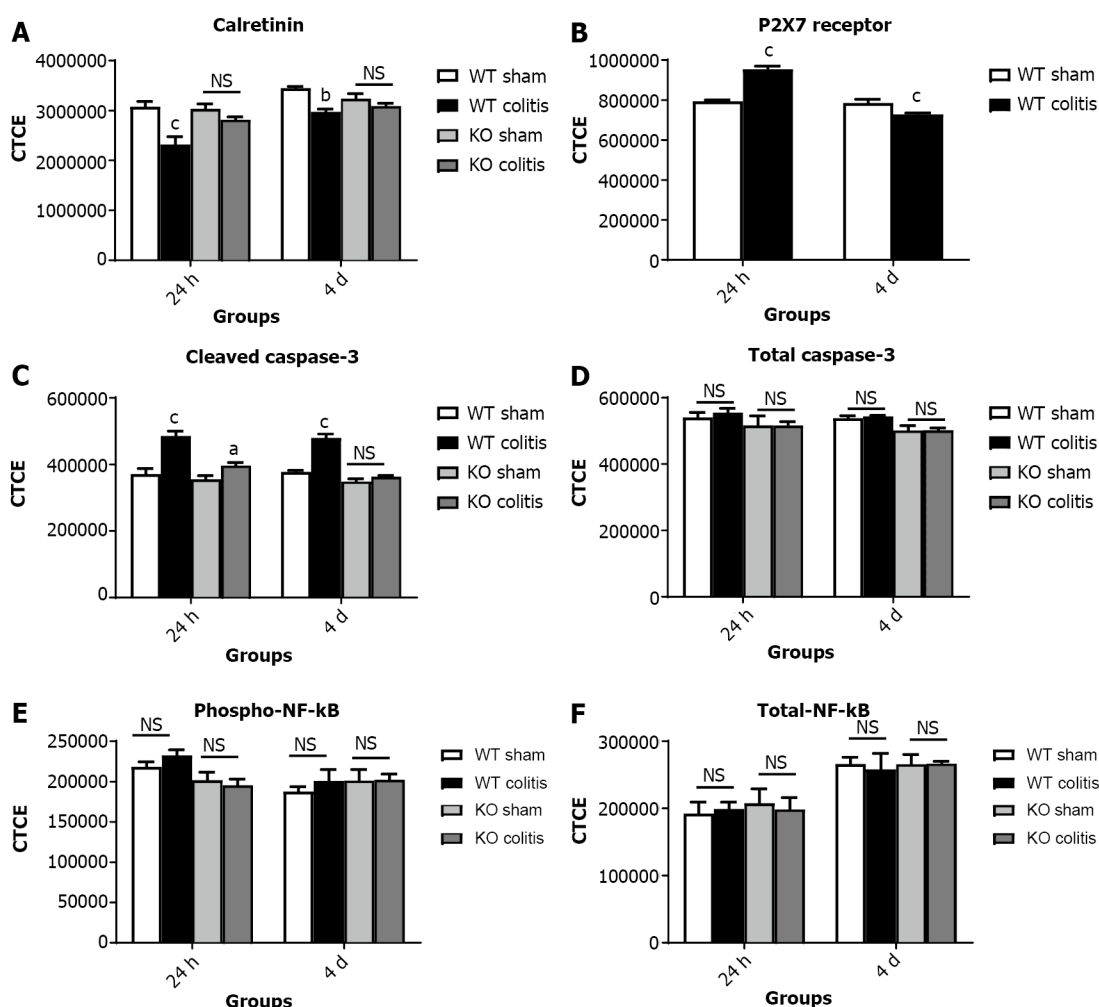
**Figure 9** Distribution frequency (%) of the profile areas. A and B: Calretinin-ir neurons; C and D: Calretinin-ir nucleus; E and F: Calretinin-ir cytoplasm in the myenteric plexus of the distal colon in mice from the wild-type (WT) sham 24 h and 4 d, WT colitis 24 h and 4 d, knockout (KO) sham 24 h and 4 d, and KO colitis 24 h and 4 d groups. WT: Wild-type; KO: Knockout.

The CTCF of P2X7 receptor-ir ganglia in the myenteric plexus of the distal colon was increased by 16.8% in the WT colitis 24 h group compared to the WT sham 24 h group ( $953784 \pm 15825$  vs  $793451 \pm 6809$ ,  $P < 0.001$ ) and decreased by 7.2% in the WT colitis 4 d group compared to the WT sham 4 d group ( $728412 \pm 6295$  vs  $785419 \pm 18143$ ,  $P < 0.01$ ). P2X7 receptor expression was not observed in the myenteric ganglia in the KO sham (24 h and 4 d) and KO colitis (24 h and 4 d) groups (Figure 10B).

The CTCF of cleaved caspase-3-ir ganglia in the myenteric plexus of the distal colon was increased by 23.6% in the WT colitis 24 h group compared to the WT sham 24 h group ( $485949 \pm 14140$  vs  $371371 \pm 16426$ ,  $P < 0.001$ ) and increased by 10.5% in the KO colitis 24 h group compared to the KO sham 24 h group ( $396888 \pm 8737$  vs  $355154 \pm 11060$ ,  $P < 0.05$ ). The CTCF of cleaved caspase-3-ir myenteric ganglia was increased by 21.2% in the WT colitis 4 d group compared to the WT sham 4 d group ( $480381 \pm 11336$  vs  $378365 \pm 4053$ ,  $P < 0.001$ ). No statistically significant difference in the CTCF of cleaved caspase-3-ir myenteric ganglia was observed between the KO colitis 4 d group and the KO sham 4 d group (Figure 10C). In addition, no statistically significant difference in the CTCF of total caspase-3-ir (Figure 10D), phospho-NF- $\kappa$ B-ir (Figure 10E) and total NF- $\kappa$ B-ir (Figure 10F) ganglia was observed between the WT colitis (24 h and 4 d) and WT sham (24 h and 4 d) groups or between the KO colitis (24 h and 4 d) and KO sham (24 h and 4 d) groups.

### Transmission electron microscopy

Transmission electron microscopy was used to assess the ultrastructural morphology of the myenteric plexus of the distal colon in mice from all groups. Myenteric neurons, neuronal nuclei and organelles, and the interaction between neurons and enteric glial cells were visualized. In the WT colitis 24 h and KO colitis 24 h groups, neurons with a necrotic phenotype characterized mainly by nuclear disruption and apparent nuclear autolysis, chromatin fragmentation and condensation, and cytoplasmic disorganization were observed. Enteric glial cells also showed morphological changes similar to those of neurons. In the WT colitis 4 d group and less frequently in the KO colitis 4 d group, neurons showed irregular nuclei and nuclear membrane invaginations. The cell membrane remained intact, and apoptotic bodies were sometimes observed. Enteric glial cells also showed features consistent with apoptosis. In the WT sham (24 h and 4 d) and KO sham (24 h and 4 d) groups, neurons showed large and round/oval nuclei and no sign of structural disruption in the cytoplasm (Figure 11).



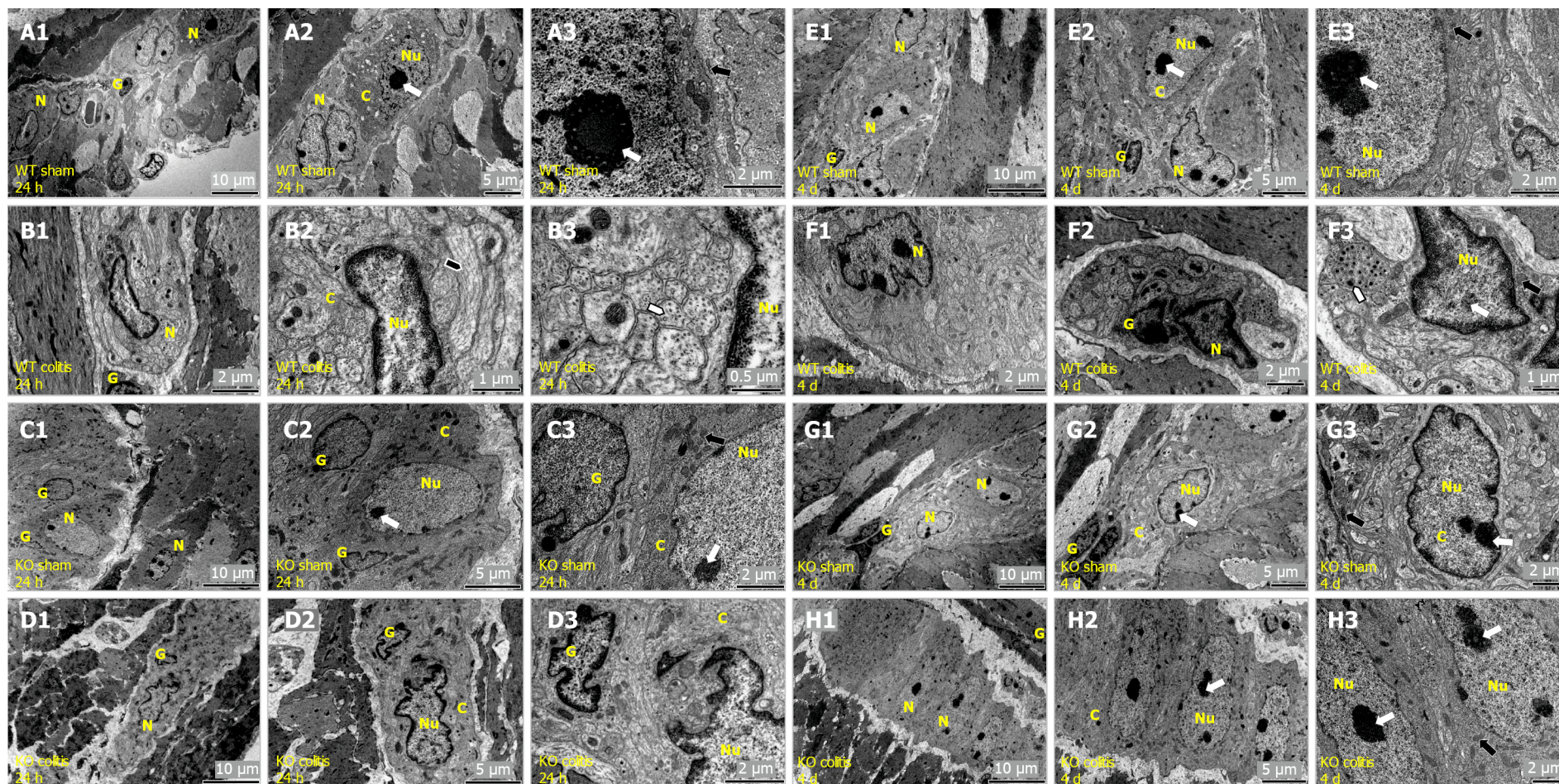
DOI: 10.3748/wjg.v29.i22.3440 Copyright ©The Author(s) 2023.

**Figure 10** Corrected total cell fluorescence of myenteric neurons. A: calretinin; B: P2X7 receptor; C: Cleaved caspase-3; D: Total caspase-3; E: Phospho-nuclear factor kappa B (NF-κB); F: Total NF-κB in the myenteric plexus of the distal colon in mice from the WT sham 24 h and 4 d, wild-type (WT) colitis 24 h and 4 d, knockout (KO) sham 24 h and 4 d, and KO colitis 24 h and 4 d groups. The data are presented as the arithmetic mean  $\pm$  SE. <sup>a</sup> $P < 0.05$  vs sham groups; <sup>b</sup> $P < 0.01$  vs sham groups; <sup>c</sup> $P < 0.001$  vs sham groups; NS: Not significant. WT: Wild-type; KO: Knockout; NF-κB: Nuclear factor kappa B.

### Histology

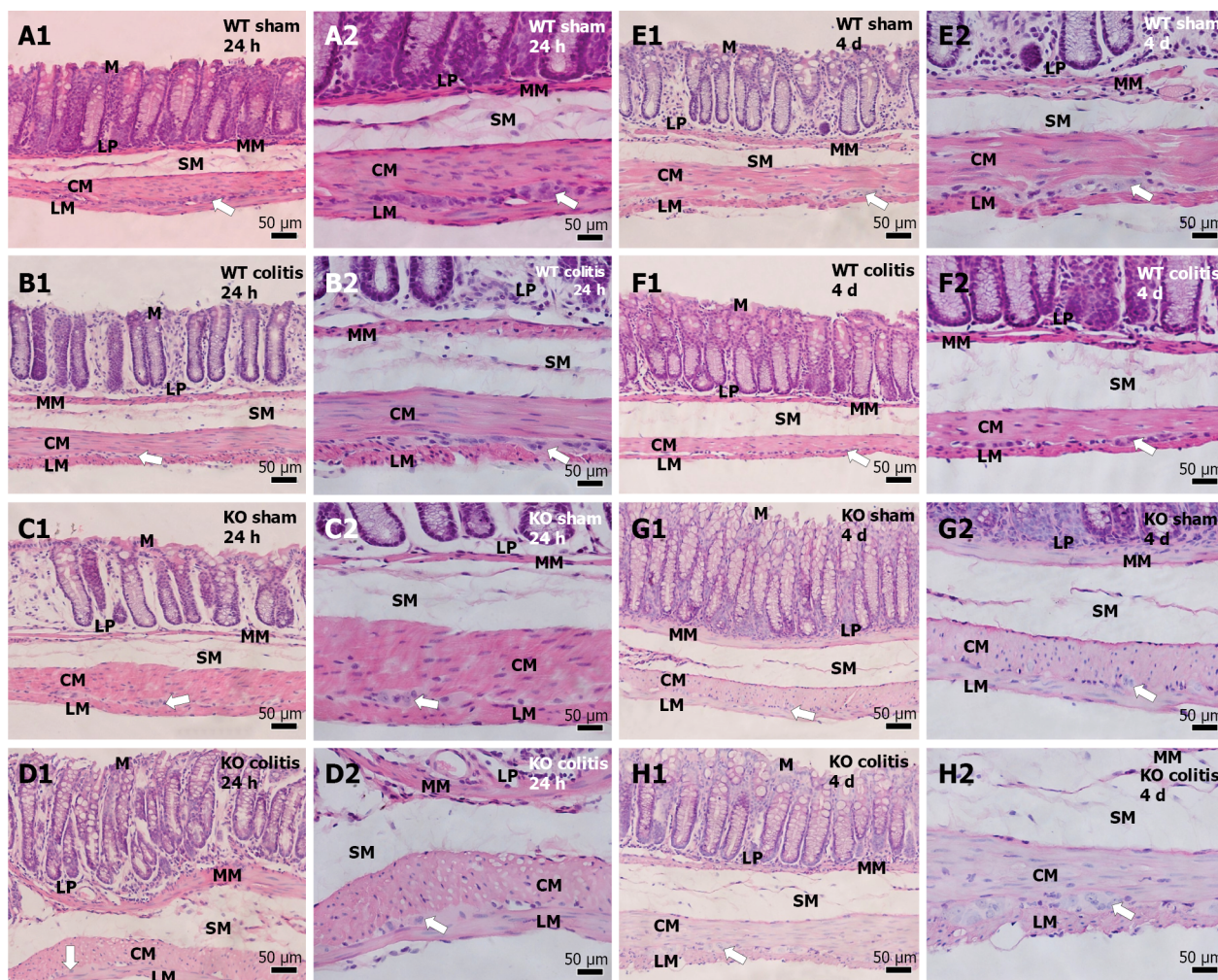
Distal colon morphology was evaluated by hematoxylin and eosin staining. In the WT sham 24 h, KO sham 24 h, WT sham 4 d, and KO sham 4 d groups, the mucosa and submucosal layers, the intestinal crypts, the lamina propria, and the longitudinal and circular muscles were intact. In the WT colitis 24 h group, tissue damage characterized by cellular disruption in the mucosal layer and thickening of the lamina propria was noted. Increased infiltration of inflammatory cells in the lamina propria and evident edema in the submucosal layer were also observed. Furthermore, the distal colon architecture was better preserved, and there were fewer inflammatory cells and less severe submucosal edema in the KO colitis 24 h, WT colitis 4 d, and KO colitis 4 d groups than in the WT colitis 24 h group (Figure 12).

Picrosirius red staining revealed the presence of thick fibers (red) in the lamina propria, in the submucosal layer, intermingled with and surrounding the muscle layer, and circumscribing the myenteric ganglia, the presence of fine fibers (green under polarized light microscopy) in the lamina propria and submucosal layer, and the presence of mixed fibers (yellow under polarized light microscopy) in all regions of the intestinal tissue in the WT sham 24 h and WT sham 4 d groups. In contrast, in the WT colitis 24 h group, the number of thick collagen fibers in the submucosal layer and around the myenteric ganglia was increased, and collagen fibers were increased in number and disorganized in the lamina propria and accumulated in the subepithelial region. In the KO sham 24 h group, greater integrity and organization of collagen fibers was visualized in the submucosal layer. In the KO colitis 24 h group, there were fewer thick collagen fibers in the lamina propria and involving the myenteric ganglia and more disordered fibers in the submucosa and subepithelial region than in the corresponding sham group. The tissue in the WT colitis 4 d group was very similar to that in the WT colitis 24 h group. However, there were more thick collagen fibers around the myenteric ganglia, and they were better organized in the submucosal layer due to more discrete local edema. Tissue



DOI: 10.3748/wjg.v29.i22.3440 Copyright ©The Author(s) 2023.

**Figure 11** Transmission electron microscopy photomicrograph showing the ultrastructural organization of the myenteric plexus of the distal colon in mice. A1-A3: Wild-type (WT) sham 24 h; B1-B3: WT colitis 24 h; C: Knockout (KO) sham 24 h; D1-D3: KO colitis 24 h; E1-E3: WT sham 4 d; F1-F3: WT colitis 4 d; G1-G3: KO sham 4 d; H1-H3: KO colitis 4 d groups. In the WT colitis 24 h and KO colitis 24 h groups, neurons with a necrotic phenotype characterized by nuclear disruption and apparent nuclear autolysis, chromatin fragmentation and condensation, and cytoplasmic disorganization were observed. Enteric glial cells also showed morphological changes. In the WT colitis 4 d group and less frequently in the KO colitis 4 d group, neurons showed irregular nuclei and nuclear membrane invaginations. The cell membrane remained intact, and apoptotic bodies were sometimes observed. Enteric glial cells also showed features consistent with cell apoptosis. In the WT sham 24 h, KO sham 24 h, WT sham 4 d and KO sham 4 d groups, neurons exhibited large and rounded/oval nuclei, and there were no signs of structural changes in the cytoplasm. N: Myenteric neuron; G: Enteric glial cells; C: Myenteric neuron cytoplasm; Nu: Myenteric neuron nucleus. Nucleolus (white arrow), mitochondria (black arrow), nuclear membrane invaginations (black arrowhead), and vesicles and microtubules (white arrowhead). WT: Wild-type; KO: Knockout.



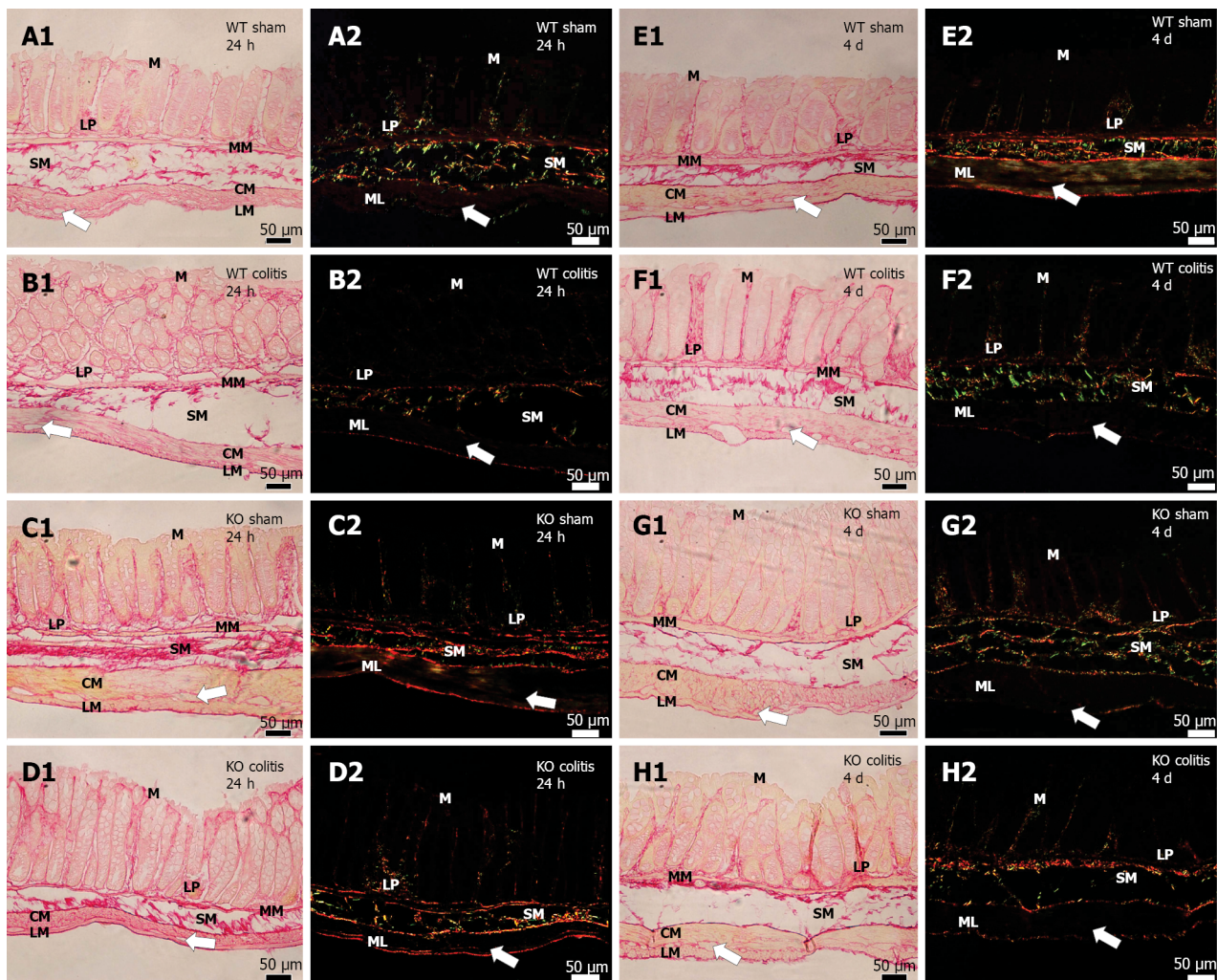
DOI: 10.3748/wjg.v29.i22.3440 Copyright ©The Author(s) 2023.

**Figure 12** Photomicrographs of hematoxylin-eosin-stained transverse sections of the distal colons of mice of different groups. A1 and A2: Wild-type (WT) sham 24 h; B1 and B2: WT colitis 24 h; C1 and C2: Knockout (KO) sham 24 h; D1 and D2: KO colitis 24 h; E1 and E2: WT sham 4 d; F1 and F2: WT colitis 4 d; G1 and G2: KO sham 4 d; H1 and H2: KO colitis 4 d groups. Tissue integrity was maintained in the sham groups, and cellular disruption and thickening of the lamina propria and submucosal layer were observed in the WT colitis group. Tissue was better preserved, and there were fewer inflammatory cells in the KO colitis group than in the WT colitis group. M: Mucosal layer; LP: Lamina propria; MM: Mucosal muscle; SM: Submucosal layer; ML: Muscle layer; CM: Circular musculature; LM: Longitudinal musculature; WT: Wild-type; KO: Knockout. White arrows mean myenteric ganglion.

architecture was similar between the KO sham 4 d and KO colitis 4 d groups and the KO sham 24 h and KO colitis 24 h groups (Figure 13).

Masson's trichome staining demonstrated that in the WT sham 24 h, KO sham 24 h, and WT sham 4 d groups, collagen fibers (blue) were present in the lamina propria and between the mucosal muscle and muscle layer (muscle fibers and cell nuclei shown in red) and enveloped the myenteric ganglia, and there were more collagen fibers throughout the submucosal layer. In the WT colitis 24 h and WT colitis 4 d groups, a greater number of collagen fibers was observed in the lamina propria, and collagen fibers were interspersed in the muscle layer. There were fewer collagen fibers in the submucosal layer, and the collagen fibers in this layer were hyperplastic and disorganized. The tissue structure in the KO colitis 24 h group was similar to that in the KO sham 24 h group, but there were fewer collagen fibers in the submucosal layer. Tissue architecture was similar between the KO sham 4 d and KO colitis 4 d groups and the WT sham 4 d and WT colitis 4 d groups; however, in both the KO sham and KO colitis groups, the collagen fibers in the submucosal layer were more organized (Figure 14).

Periodic acid-Schiff staining was performed to evaluate the presence and morphology of goblet cells in the distal colon. In the WT sham 24 h and WT sham 4 d groups, goblet cells in the distal colon were present throughout the epithelium, typically showed a columnar or oval shape and were circular when filled with mucus. In the WT colitis 24 h group, these cells were present in smaller quantities, were reduced in size, and presented a more rounded shape with an intumescent appearance. On the other hand, in the KO sham 24 h and KO colitis 24 h groups, the number of goblet cells was apparently increased. In the KO sham 24 h group, the cells were similar in size to those in the WT sham group, and in the KO colitis 24 h group, there was a more heterogeneous cell population. In the WT colitis 4 d group, goblet cells were apparently increased in number but still reduced in size. However, larger cells



DOI: 10.3748/wjg.v29.i22.3440 Copyright ©The Author(s) 2023.

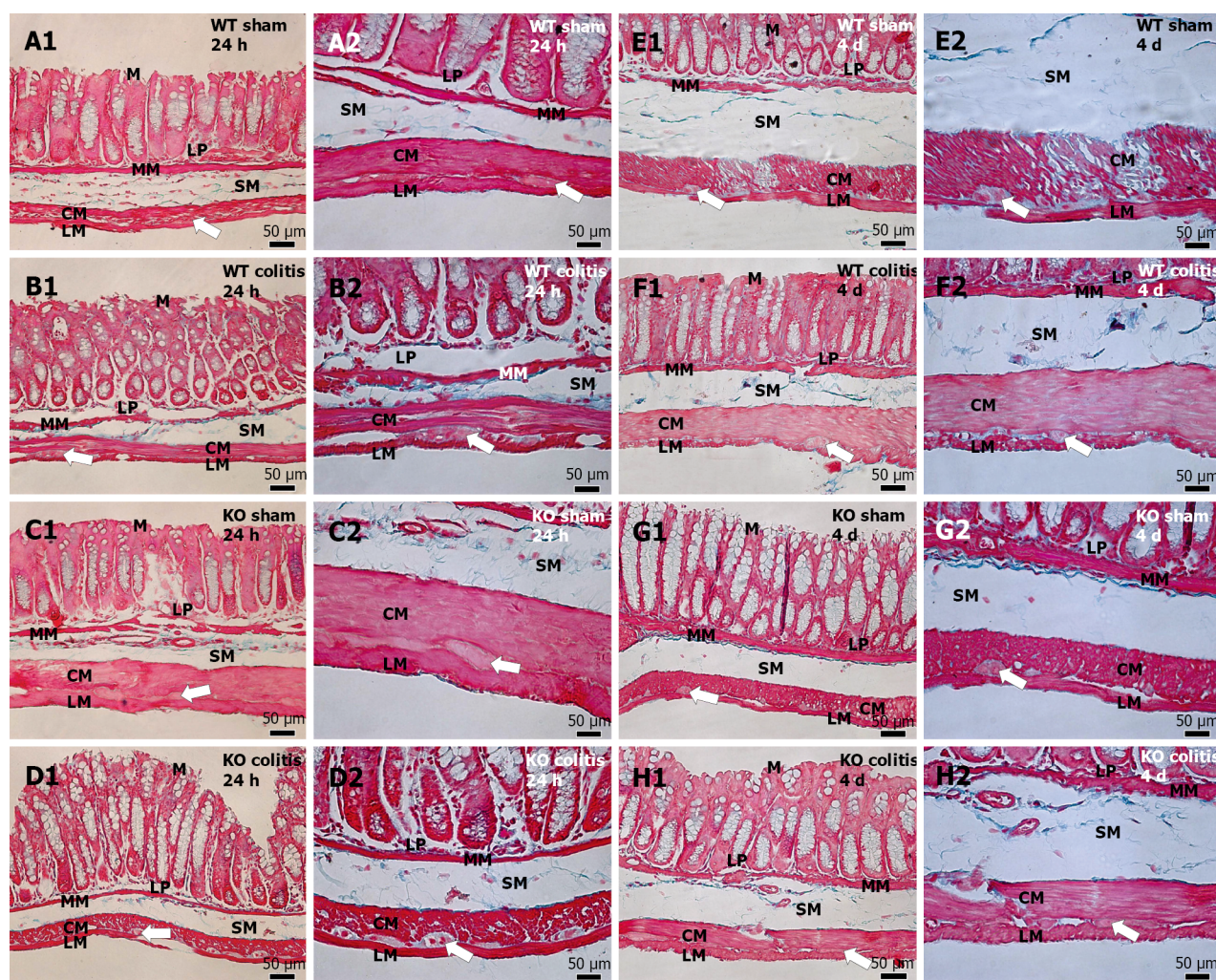
**Figure 13** Photomicrograph of picosirius red-stained transverse sections of the distal colons of mice of different groups. A1 and A2: Wild-type (WT) sham 24 h; B1 and B2: WT colitis 24 h; C1 and C2: Knockout (KO) sham 24 h; D1 and D2: KO colitis 24 h; E1 and E2: WT sham 4 d; F1 and F2: WT colitis 4 d; G1 and G2: KO sham 4 d; H1 and H2: KO colitis 4 d groups taken under an optical light (red) or polarized light (green) microscope. Thick collagen fibers (red) in the lamina propria and submucosal layer, intermingled with and involving the muscle layer, and circumscribing the myenteric ganglia were observed in the sham groups. In the WT colitis group, there was a decrease in the number of these fibers in the submucosal layer and around the myenteric ganglia, an increase in the number and disorganization of these fibers in the lamina propria and accumulation of these fibers in the subepithelial region. Tissue was better preserved in the KO colitis group. M: Mucosal layer; LP: Lamina propria; MM: Mucosal muscle; SM: Submucosal layer; ML: Muscle layer; CM: Circular musculature; LM: Longitudinal musculature; WT: Wild-type; KO: Knockout. White arrows mean myenteric ganglion.

were also observed near the surface of the intestinal crypts. Finally, there was a notable increase in the number of goblet cells in the distal colon in the KO sham 4 d and KO colitis 4 d groups (Figure 15).

**Number of goblet cells per intestinal crypt:** The number of goblet cells per intestinal crypt in the distal colon was decreased by 37.6% in the WT colitis 24 h group compared to the WT sham 24 h group ( $8.63 \pm 0.43$  vs  $13.84 \pm 1.00$ ,  $P < 0.01$ ). No statistically significant differences in the goblet cell density were observed between the KO colitis (24 h and 4 d) groups and the KO sham (24 h and 4 d) groups, but the goblet cell density was significantly different between the WT and KO groups ( $P < 0.001$ ). In the KO groups, there was a greater number of goblet cells per intestinal crypt (Figure 16).

## DISCUSSION

Despite the large amount of research on IBDs, the pathogenesis of these diseases is still unclear[74,75]. However, it is known that changes in the interaction between immune cells and the gut microbiota may contribute to the clinical progression of IBDs[76-80] and that nonimmune components may alter cellular structure and function in response to inflammation[81]. Indeed, recent evidence has indicated that colitis affects not only the intestinal mucosa but also the muscle layer and components of the ENS. Hence, gastrointestinal symptoms result from degenerative changes and a reduction in the number of



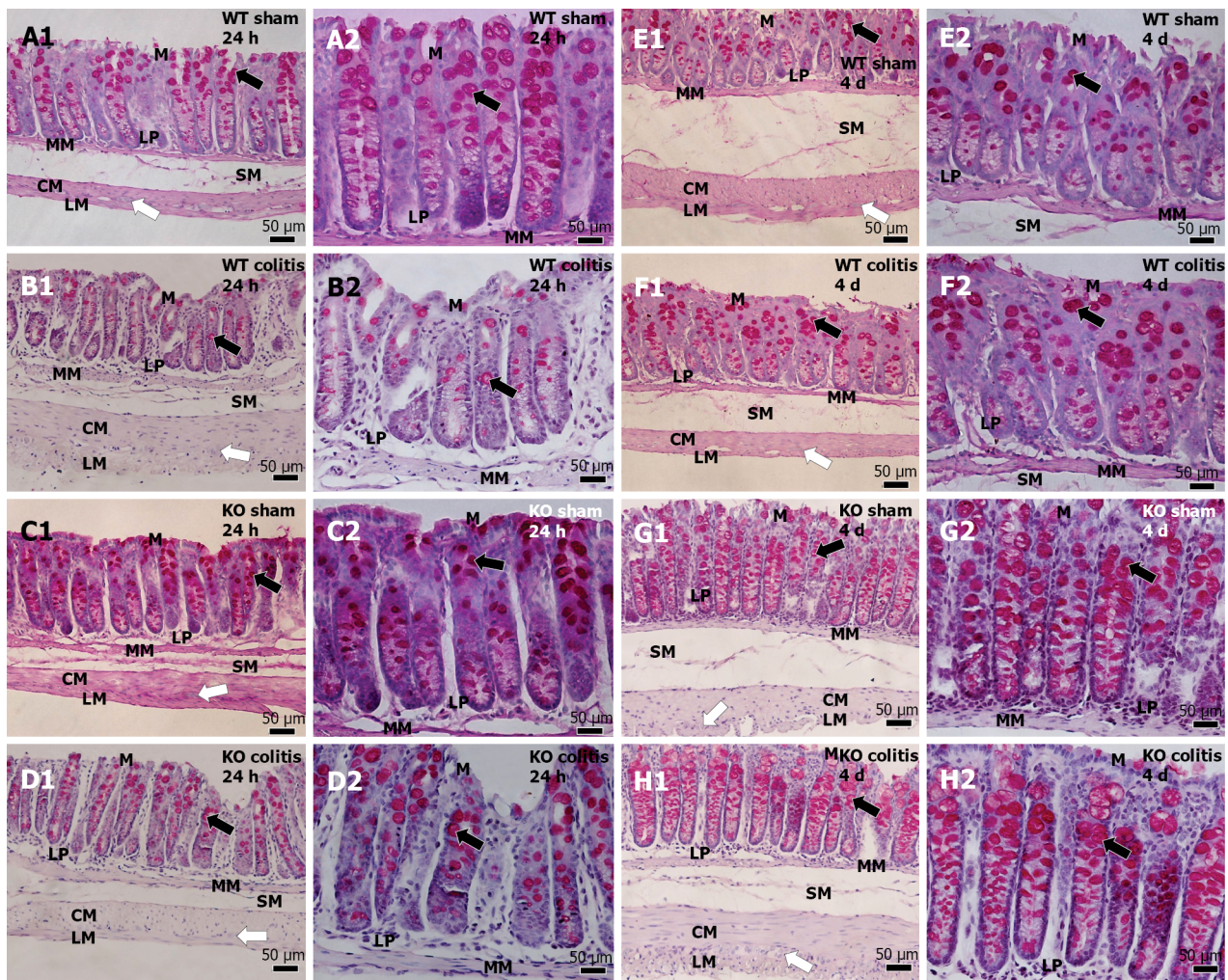
DOI: 10.3748/wjg.v29.i22.3440 Copyright ©The Author(s) 2023.

**Figure 14** Photomicrographs of Masson's trichrome-stained transverse sections of the distal colons of mice in different groups. A1 and A2: Wild-type (WT) sham 24 h; B1 and B2: WT colitis 24 h; C1 and C2: Knockout (KO) sham 24 h; D1 and D2: KO colitis 24 h; E1 and E2: WT sham 4 d; F1 and F2: WT colitis 4 d; G1 and G2: KO sham 4 d; H1 and H2: KO colitis 4 d groups. Collagen fibers (blue) in the lamina propria and submucosal layer, intermingled with and involving the muscle layer, and circumscribing the myenteric ganglia were observed in the sham groups. In the WT colitis group, there was a decrease in the number of these fibers in the submucosal layer, and the collagen fibers in this layer were hyperplastic and disorganized. Moreover, the number of collagen fibers was increased in the lamina propria, and collagen fibers were intermingled in the muscular layer. Tissue was better preserved in the KO colitis group. WT: Wild-type; KO: Knockout; M: Mucosal layer; LP: Lamina propria; MM: Muscularis mucosae; SM: Submucosal layer; LM: Longitudinal muscle; CM: Circular muscle; LM: Longitudinal musculature; White arrows: Myenteric ganglion.

enteric neurons and glial cells, sometimes induced by the P2X7 receptor[35-40,48,50,62,63,82-84]. However, little is known about the cellular signaling mechanisms responsible for the loss of enteric innervation in IBDs[85].

In the present study, we hypothesized that the loss of myenteric neurons resulting from TNBS-induced colitis is related to cell death pathways mediated by caspase-3 and NF- $\kappa$ B-mediated transcription. In addition, we hypothesized that KO animals would be less affected by administration of an inflammatory stimulus. We compared pathological changes at two different time points after colitis induction. At both 24 h and four days post-inflammatory stimulus administration, there was a significant reduction in the number of myenteric neurons in the WT groups but not in the KO groups. In addition, the neuronal area was increased in the WT colitis 24 h and KO colitis 24 h groups, and this change was due to an increase in the cytoplasmic area; however, a decrease in the cytoplasmic area along with nuclear shrinkage was observed in the WT colitis 4 d group. We also demonstrated that when the P2X7 receptor was knocked out and at four days after colitis induction, the infiltration of inflammatory cells and microscopic tissue damage were attenuated, indicating that disease symptoms evolved during the experimental period.

According to Brenna *et al*[86], the TNBS-induced colitis model is a suitable model for studying biological processes associated with IBDs and can provide clinically relevant data; moreover, there are well-established protocols for constructing this model in both rats and mice[38-40,86-92]. Furthermore, KO animals have been used to study the onset and development of these disorders[83,86,93,94];



DOI: 10.3748/wjg.v29.i22.3440 Copyright ©The Author(s) 2023.

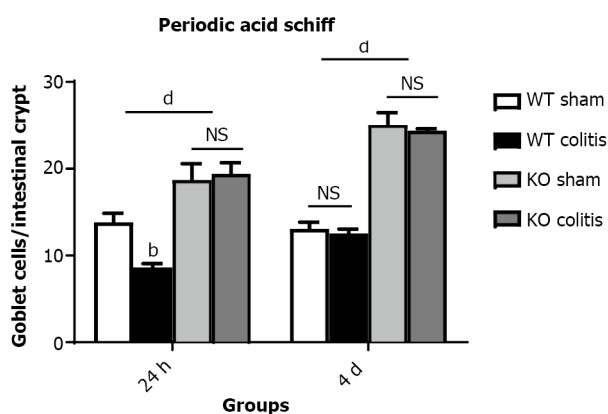
**Figure 15** Photomicrograph of periodic acid Schiff-stained transverse sections of the distal colons of mice. A1 and A2: Wild-type (WT) sham 24 h; B1 and B2: WT colitis 24 h; C1 and C2: Knockout (KO) sham 24 h; D1 and D2: KO colitis 24 h; E1 and E2: WT sham 4 d; F1 and F2: WT colitis 4 d; G1 and G2: KO sham 4 d; H1 and H2: KO colitis 4 d groups. Goblet cells were observed throughout the epithelium in the sham groups, and there was an apparent reduction in goblet cell number and size in the WT colitis group. In addition, goblet cells showed a more rounded shape and an intumescent appearance in the WT colitis group. In the KO groups, an apparent increase in the number of goblet cells was noted. WT: Wild-type; KO: Knockout; M: Mucosal layer; LP: Lamina propria; MM: Mucosal muscle; SM: Submucosal layer; ML: Muscle layer; CM: Circular musculature; LM: Longitudinal musculature; white arrows: Myenteric ganglion; black arrows: Goblet cells.

however, the degree of similarity between experimentally induced colitis and spontaneous colitis in humans is still unclear[86].

In the present study, we recorded body weight and the change in DAI daily. After euthanasia, the macro- and microscopic lesions in the distal colon were characterized[64-67]. The colitis model animals lost more weight on the first day but recovered on the subsequent days. It is worth noting that in the colitis model groups, there were also greater changes in stool consistency and the presence of blood in the stool. Similarly, tissue hyperemia was noted only in the colitis groups, and the WT colitis 24 h group exhibited more severe microscopic damage. The absence of statistically significant differences in phenotype between the KO sham and KO colitis groups is consistent with previous literature showing that KO of the P2X7 receptor provides greater protection against inflammation[52,56,83,93,94].

It was previously demonstrated that intestinal inflammation induces changes in the density of neurons expressing different chemical codes in the ENS and that these changes vary between animal models and human patients. It is known that the number of neurons is reduced 24 h to seven days after the induction of colitis[35-40,62,81,89,95]. It has been reported that this decrease in the number of neurons occurs as early as six hours after colitis induction[35,81] and that, as observed in the present study, this decrease is already significant at 24 h.

According to Sanovic *et al*[81], the number of enteric neurons continues to decrease from the second to the fourth day and remains constant until day 35, suggesting that enteric neuron loss is long lasting and irreversible. Similarly, Linden *et al*[95] also reported that the number of neurons is not yet recovered at 56 d after colitis induction. In contrast, Poli *et al*[96] observed that at 30 d after inflammation



DOI: 10.3748/wjg.v29.i22.3440 Copyright ©The Author(s) 2023.

**Figure 16** Number of goblet cells per intestinal crypt of the distal colon in mice from the wild-type sham 24 h and 4 d, wild-type colitis 24 h and 4 d, knockout sham 24 h and 4 d, and knockout colitis 24 h and 4 d groups. The data are presented as the arithmetic mean  $\pm$  SE. <sup>b</sup> $P < 0.01$  vs sham groups; <sup>d</sup> $P < 0.001$  vs wild-type groups; NS: Not significant. WT: Wild-type; KO: Knockout.

induction, the myenteric plexus showed similar labeling to that in the control group. In our study, there was a slight increase in the number of calcitonin-ir neurons in the WT colitis 4 d and KO colitis 4 d groups compared with the WT sham 24 h and KO sham 24 h groups, which may indicate that neurons exhibit some degree of plasticity in response to inflammatory injury. Despite this apparent alleviation of pathological changes after the inflammatory stimulus is removed, neuronal damage and activation of signaling pathways that potentially lead to cell death have already occurred.

The neuronal area was significantly increased in the WT colitis 24 h and KO colitis 24 h groups compared to the WT sham 24 h and KO sham 24 h groups, and this change was due to an increase in the cytoplasmic area. On the other hand, a significant reduction in neuronal area accompanied by a reduction in nuclear area was observed in the WT colitis 4 d group. In addition, ultrastructural analysis of myenteric neurons revealed nuclear disruption and cytoplasmic disorganization in the 24 h WT colitis and 24 h KO colitis groups and nuclear membrane folding associated with the formation of apoptotic bodies in the 4 d WT colitis group. Thus, neurons first underwent necrosis characterized by massive cell death and then, after four days, underwent apoptosis characterized by cytoplasmic condensation and nuclear shrinkage[4,6-8,10,14,35,82,97].

As reported by Martin[1] and Kanduc *et al*[2], cell death can occur either through necrosis or apoptosis and results from the activation of intrinsic death programs or passive disruption of the cell membrane resulting from damaging environmental stimuli[10]. In necrosis, the death stimulus alone causes the loss of the cell[4], whereas in apoptosis, a cascade of events that orchestrate destruction of the cell in a controlled manner is activated. The main effector of both processes is caspase-3[4,8,10,45,98], a protease that when activated fragments DNA and disrupts cellular organization and leads to cell death [4,7,98-101].

From the CTCF analysis, a greater intensity of cleaved caspase-3 was observed in the 24 h WT colitis, 24 h KO colitis and 4 d WT colitis groups, indicating a higher activation of myenteric neuron pathway death. Indeed, these results are in line with the decrease in enteric neuronal density arising from colitis. In addition, we observed a higher fluorescence of the P2X7 receptor in the WT colitis 24 h group, suggesting its greater activation during the inflammatory process[52,54,60,93,102-104].

According to North[105], Burnstock[106], and DUBYAK[107], constant stimulation of the P2X7 receptor *via* ATP results in the efflux of  $K^+$  and the influx of  $Ca^{2+}$  and  $Na^+$  and triggers the formation of a nonselective membrane pore that makes the cell permeable to molecules of up to 900 daltons. Because of this imbalance, specific phospholipases and kinases that, in addition to exerting other effects, can trigger the caspase cascade are activated. As a result, the activation of the transcription factor NF- $\kappa$ B leads to the expression of proinflammatory genes and stimulates both inflammation and cell death. It has also been found that ATP is released *via* the panexin-1 channel[37,49,50], and the extracellular increase in ATP indicates exacerbation of inflammation[56,60], increased P2X7 receptor activation and severe neuronal death[37,51,52,56,103].

Consistent with the findings presented above, our results showed that in KO mice, myenteric calcitonin-ir neurons were protected to a greater extent, and the loss of this receptor obviously prevented its activation, inhibiting the subsequent cascade of events culminating in cell death. Despite this, a decrease in the number of myenteric neurons was observed in the KO colitis 24 h group compared to the KO sham 24 h group, which suggests that neuronal protection and cell death also involve pathways not linked to the P2X7 receptor[4,7,8,45,47].

Our results are in line with what has been reported in the literature and confirm that neuronal death mediated by caspase-3 activation is related to purinergic signaling *via* the P2X7 receptor in the

myenteric plexus of mice with TNBS-induced colitis. However, it is worth noting that NF- $\kappa$ B plays a role in IBDs[108-111], but its activation is minimal during the inflammatory process[112].

Histologically, inflammatory infiltration, tissue damage, and loss of goblet cells in intestinal tissue were attenuated at four days compared with 24 h after colitis induction. This finding is consistent with the alleviation of symptoms observed in the colitis groups since the inflammatory stimulus was removed and corroborates the findings reported in the literature demonstrating that tissue recovery indicates better clinical outcomes[113,114]. Nevertheless, in the WT colitis 4 d group, collagen fibers in the lamina propria were increased in number and disorganized, indicating that the fibrosis in the mucosal layer[38,52,115,116] observed at 24 h did not decrease. On the other hand, KO animals always showed milder tissue injury and better recovery than WT animals.

It is possible that the reduction in the number of goblet cells observed in the colitis groups aggravated acute intestinal inflammation; this phenomenon has already been reported both in experimental animals and in human patients[38,52,83,117-120]. However, even though these cells play a critical role in maintaining a physical barrier by producing mucus in the gut[117,121-123], it is unclear whether the loss of their function contributes to the onset of inflammation or is a consequence of it[117]. The results of our study indicated that colitis induced the loss of these cells, and tissue recovery was observed at four days, as indicated by an increased number of goblet cells that grew as they emerged from the basal lamina and moved toward the epithelial surface. The increase in cell proliferation in the KO groups[94], which resulted in the increase in the number of goblet cells, may have also protected the mucosa by leading to increased mucus production. As reported by Van der Sluis *et al*[121], Niv[124], and Grondin *et al*[123], deficiencies in the production of diverse types of mucins favor the onset and progression of intestinal inflammation.

## CONCLUSION

In conclusion, we demonstrate that although the distal colons of mice with colitis showed good histological recovery, neuronal injury occurred in the myenteric plexus and probably impaired intestinal function. Studies in which animals are maintained for a longer period of time seem to be needed to elucidate the effects of P2X7 signaling on long-term neuronal survival. Moreover, it was confirmed that the P2X7 receptor is closely associated with neuronal necrosis and apoptosis dependent on the caspase-3 pathway but not on NF- $\kappa$ B. KO animals were less affected by ulcerative colitis. Thus, the P2X7 receptor may be a potential therapeutic target for IBDs.

## ARTICLE HIGHLIGHTS

### Research background

Inflammation affects enteric neurons and has P2X7 receptor signaling.

### Research motivation

The motivation of the work was to study the mechanisms of nuclear factor kappa B (NF- $\kappa$ B) and caspase-3.

### Research objectives

To study calretinin-positive neurons and caspase-3 and NF- $\kappa$ B pathways in intestinal inflammation.

### Research methods

Research methods of immunohistochemistry, morphometry, conventional histology and transmission electron microscopy were used.

### Research results

There was a decrease in calretinin neurons in wild type colitis (WT) animals and recovery of neurons in mice deficient for the P2X7 receptor (KO). There was an increase in caspase-3 and NF- $\kappa$ B pathways in the WT colitis and recovery animals in the KO groups.

### Research conclusions

The P2X7 receptor is involved in the decrease of neurons in the WT colitis group, and this receptor could be a therapeutic target.

### Research perspectives

The perspective of the work is to use other techniques to explain other pathways of action mechanisms.

## FOOTNOTES

**Author contributions:** Magalhães HIR was responsible for the literature review and analysis and wrote the manuscript; Machado FA, Souza RF, Caetano MAF, Figliuolo VR, and Coutinho-Silva R helped with acquisition, analysis and interpretation of data and made critical suggestions about the writing; Castelucci P designed the study, helped with acquisition, analysis and interpretation of data, performed the critical interpretation and revised the manuscript for intellectual content; and all authors approved the final version of the manuscript.

**Supported by** the National Council for Scientific and Technological Development, No. 168015/2018-8; and the São Paulo Research Foundation, No. 2014/25927-2 and No. 2018/07862-1.

**Institutional review board statement:** The study was reviewed and approved by the pela Comissão de Ética no Uso de Animais da Instituto de Ciências Biomédicas Universidade de São Paulo (Approval No. CEUA 2372300921).

**Institutional animal care and use committee statement:** All procedures involving animals were reviewed and approved by the Ethic Committee on Animal Use of the School of Veterinary Medicine and Animal Science University of São Paulo (Approval No. CEUA 2841270120).

**Conflict-of-interest statement:** The authors have no conflicts of interest.

**Data sharing statement:** Technical appendix, statistical code, and dataset available from the corresponding author at [pcastel@usp.br](mailto:pcastel@usp.br). Participants gave informed consent for data sharing.

**ARRIVE guidelines statement:** The authors have read the ARRIVE Guidelines, and the manuscript was prepared and revised according to the ARRIVE Guidelines.

**Open-Access:** This article is an open-access article that was selected by an in-house editor and fully peer-reviewed by external reviewers. It is distributed in accordance with the Creative Commons Attribution NonCommercial (CC BY-NC 4.0) license, which permits others to distribute, remix, adapt, build upon this work non-commercially, and license their derivative works on different terms, provided the original work is properly cited and the use is non-commercial. See: <https://creativecommons.org/licenses/by-nc/4.0/>

**Country/Territory of origin:** Brazil

**ORCID number:** Henrique Inhauser Riceti Magalhães [0000-0001-9151-8160](https://orcid.org/0000-0001-9151-8160); Roberta Figueiroa Souza [0000-0003-4380-6373](https://orcid.org/0000-0003-4380-6373); Marcos Antônio Ferreira Caetano [0000-0002-9981-3241](https://orcid.org/0000-0002-9981-3241); Patricia Castelucci [0000-0002-7475-5962](https://orcid.org/0000-0002-7475-5962).

**Corresponding Author's Membership in Professional Societies:** American Gastroenterological Association, No. C-1029455.

**S-Editor:** Chen YL

**L-Editor:** A

**P-Editor:** Chen YL

## REFERENCES

- Martin LJ. Neuronal cell death in nervous system development, disease, and injury (Review). *Int J Mol Med* 2001; **7**: 455-478 [PMID: [11295106](https://pubmed.ncbi.nlm.nih.gov/11295106/) DOI: [10.3892/ijmm.7.5.455](https://doi.org/10.3892/ijmm.7.5.455)]
- Kanduc D, Mittelman A, Serpico R, Sinigaglia E, Sinha AA, Natale C, Santacroce R, Di Corcia MG, Lucchese A, Dini L, Pani P, Santacroce S, Simone S, Bucci R, Farber E. Cell death: apoptosis versus necrosis (review). *Int J Oncol* 2002; **21**: 165-170 [PMID: [12063564](https://pubmed.ncbi.nlm.nih.gov/12063564/) DOI: [10.3892/ijo.21.1.165](https://doi.org/10.3892/ijo.21.1.165)]
- Leist M, Jäättelä M. Four deaths and a funeral: from caspases to alternative mechanisms. *Nat Rev Mol Cell Biol* 2001; **2**: 589-598 [PMID: [11483992](https://pubmed.ncbi.nlm.nih.gov/11483992/) DOI: [10.1038/35085008](https://doi.org/10.1038/35085008)]
- Friedlander RM. Apoptosis and caspases in neurodegenerative diseases. *N Engl J Med* 2003; **348**: 1365-1375 [PMID: [12672865](https://pubmed.ncbi.nlm.nih.gov/12672865/) DOI: [10.1056/NEJMr022366](https://doi.org/10.1056/NEJMr022366)]
- Dong Z, Saikumar P, Weinberg JM, Venkatachalam MA. Calcium in cell injury and death. *Annu Rev Pathol* 2006; **1**: 405-434 [PMID: [18039121](https://pubmed.ncbi.nlm.nih.gov/18039121/) DOI: [10.1146/annurev.pathol.1.110304.100218](https://doi.org/10.1146/annurev.pathol.1.110304.100218)]
- Kerr JF, Wyllie AH, Currie AR. Apoptosis: a basic biological phenomenon with wide-ranging implications in tissue kinetics. *Br J Cancer* 1972; **26**: 239-257 [PMID: [4561027](https://pubmed.ncbi.nlm.nih.gov/4561027/) DOI: [10.1038/bjc.1972.33](https://doi.org/10.1038/bjc.1972.33)]
- Hengartner MO. The biochemistry of apoptosis. *Nature* 2000; **407**: 770-776 [PMID: [11048727](https://pubmed.ncbi.nlm.nih.gov/11048727/) DOI: [10.1038/35037710](https://doi.org/10.1038/35037710)]
- Mattson MP. Apoptosis in neurodegenerative disorders. *Nat Rev Mol Cell Biol* 2000; **1**: 120-129 [PMID: [11253364](https://pubmed.ncbi.nlm.nih.gov/11253364/) DOI: [10.1038/35040009](https://doi.org/10.1038/35040009)]
- Hotchkiss RS, Strasser A, McDunn JE, Swanson PE. Cell death. *N Engl J Med* 2009; **361**: 1570-1583 [PMID: [19828534](https://pubmed.ncbi.nlm.nih.gov/19828534/) DOI: [10.1056/NEJMr0901217](https://doi.org/10.1056/NEJMr0901217)]
- Zhang Y, Chen X, Gueydan C, Han J. Plasma membrane changes during programmed cell deaths. *Cell Res* 2018; **28**: 9-21 [PMID: [29076500](https://pubmed.ncbi.nlm.nih.gov/29076500/) DOI: [10.1038/cr.2017.133](https://doi.org/10.1038/cr.2017.133)]

- 11 **Zong WX**, Thompson CB. Necrotic death as a cell fate. *Genes Dev* 2006; **20**: 1-15 [PMID: 16391229 DOI: 10.1101/gad.1376506]
- 12 **Golstein P**, Kroemer G. Cell death by necrosis: towards a molecular definition. *Trends Biochem Sci* 2007; **32**: 37-43 [PMID: 17141506 DOI: 10.1016/j.tibs.2006.11.001]
- 13 **D'Amelio M**, Cavallucci V, Cecconi F. Neuronal caspase-3 signaling: not only cell death. *Cell Death Differ* 2010; **17**: 1104-1114 [PMID: 19960023 DOI: 10.1038/cdd.2009.180]
- 14 **Yuan J**, Najafov A, Py BF. Roles of Caspases in Necrotic Cell Death. *Cell* 2016; **167**: 1693-1704 [PMID: 27984721 DOI: 10.1016/j.cell.2016.11.047]
- 15 **D'Arcy MS**. Cell death: a review of the major forms of apoptosis, necrosis and autophagy. *Cell Biol Int* 2019; **43**: 582-592 [PMID: 30958602 DOI: 10.1002/cbin.11137]
- 16 **Gorman AM**. Neuronal cell death in neurodegenerative diseases: recurring themes around protein handling. *J Cell Mol Med* 2008; **12**: 2263-2280 [PMID: 18624755 DOI: 10.1111/j.1582-4934.2008.00402.x]
- 17 **Nixon RA**, Yang DS. Autophagy and neuronal cell death in neurological disorders. *Cold Spring Harb Perspect Biol* 2012; **4** [PMID: 22983160 DOI: 10.1101/cshperspect.a008839]
- 18 **Emery E**, Aldana P, Bunge MB, Puckett W, Srinivasan A, Keane RW, Bethea J, Levi AD. Apoptosis after traumatic human spinal cord injury. *J Neurosurg* 1998; **89**: 911-920 [PMID: 9833815 DOI: 10.3171/jns.1998.89.6.0911]
- 19 **Fink KB**, Andrews LJ, Butler WE, Ona VO, Li M, Bogdanov M, Endres M, Khan SQ, Namura S, Stieg PE, Beal MF, Moskowitz MA, Yuan J, Friedlander RM. Reduction of post-traumatic brain injury and free radical production by inhibition of the caspase-1 cascade. *Neuroscience* 1999; **94**: 1213-1218 [PMID: 10625061 DOI: 10.1016/s0306-4522(99)00345-0]
- 20 **Beattie MS**, Hermann GE, Rogers RC, Bresnahan JC. Cell death in models of spinal cord injury. *Prog Brain Res* 2002; **137**: 37-47 [PMID: 12440358 DOI: 10.1016/s0079-6123(02)37006-7]
- 21 **Ekshyyan O**, Aw TY. Apoptosis in acute and chronic neurological disorders. *Front Biosci* 2004; **9**: 1567-1576 [PMID: 14977568 DOI: 10.2741/1357]
- 22 **Che Mohd Nassir CMN**, Zolkefley MKI, Ramli MD, Norman HH, Abdul Hamid H, Mustapha M. Neuroinflammation and COVID-19 Ischemic Stroke Recovery-Evolving Evidence for the Mediating Roles of the ACE2/Angiotensin-(1-7)/Mas Receptor Axis and NLRP3 Inflammasome. *Int J Mol Sci* 2022; **23** [PMID: 35328506 DOI: 10.3390/ijms23063085]
- 23 **Xu Y**, Hu Y, Xu S, Liu F, Gao Y. Exosomal microRNAs as Potential Biomarkers and Therapeutic Agents for Acute Ischemic Stroke: New Expectations. *Front Neurol* 2021; **12**: 747380 [PMID: 35173663 DOI: 10.3389/fneur.2021.747380]
- 24 **Friedlander RM**, Brown RH, Gagliardini V, Wang J, Yuan J. Inhibition of ICE slows ALS in mice. *Nature* 1997; **388**: 31 [PMID: 9214497 DOI: 10.1038/40299]
- 25 **Gervais FG**, Xu D, Robertson GS, Vaillancourt JP, Zhu Y, Huang J, LeBlanc A, Smith D, Rigby M, Shearman MS, Clarke EE, Zheng H, Van Der Ploeg LH, Ruffolo SC, Thornberry NA, Xanthoudakis S, Zamboni RJ, Roy S, Nicholson DW. Involvement of caspases in proteolytic cleavage of Alzheimer's amyloid-beta precursor protein and amyloidogenic A beta peptide formation. *Cell* 1999; **97**: 395-406 [PMID: 10319819 DOI: 10.1016/s0092-8674(00)80748-5]
- 26 **Li M**, Ona VO, Guégan C, Chen M, Jackson-Lewis V, Andrews LJ, Olszewski AJ, Stieg PE, Lee JP, Przedborski S, Friedlander RM. Functional role of caspase-1 and caspase-3 in an ALS transgenic mouse model. *Science* 2000; **288**: 335-339 [PMID: 10764647 DOI: 10.1126/science.288.5464.335]
- 27 **Okouchi M**, Ekshyyan O, Maracine M, Aw TY. Neuronal apoptosis in neurodegeneration. *Antioxid Redox Signal* 2007; **9**: 1059-1096 [PMID: 17571960 DOI: 10.1089/ars.2007.1511]
- 28 **Verma M**, Lizama BN, Chu CT. Excitotoxicity, calcium and mitochondria: a triad in synaptic neurodegeneration. *Transl Neurodegener* 2022; **11**: 3 [PMID: 35078537 DOI: 10.1186/s40035-021-00278-7]
- 29 **Palombit K**, Mendes CE, Tavares-de-Lima W, Silveira MP, Castelucci P. Effects of ischemia and reperfusion on subpopulations of rat enteric neurons expressing the P2X7 receptor. *Dig Dis Sci* 2013; **58**: 3429-3439 [PMID: 23990036 DOI: 10.1007/s10620-013-2847-y]
- 30 **Marosti AR**, da Silva MV, Palombit K, Mendes CE, Tavares-de-Lima W, Castelucci P. Differential effects of intestinal ischemia and reperfusion in rat enteric neurons and glial cells expressing P2X2 receptors. *Histol Histopathol* 2015; **30**: 489-501 [PMID: 25400134 DOI: 10.14670/HH-30.489]
- 31 **Mendes CE**, Palombit K, Vieira C, Silva I, Correia-de-Sá P, Castelucci P. The Effect of Ischemia and Reperfusion on Enteric Glial Cells and Contractile Activity in the Ileum. *Dig Dis Sci* 2015; **60**: 2677-2689 [PMID: 25917048 DOI: 10.1007/s10620-015-3663-3]
- 32 **Mendes CE**, Palombit K, Tavares-de-Lima W, Castelucci P. Enteric glial cells immunoreactive for P2X7 receptor are affected in the ileum following ischemia and reperfusion. *Acta Histochem* 2019; **121**: 665-679 [PMID: 31202513 DOI: 10.1016/j.acthis.2019.06.001]
- 33 **Palombit K**, Mendes CE, Tavares-de-Lima W, Barreto-Chaves ML, Castelucci P. Blockage of the P2X7 Receptor Attenuates Harmful Changes Produced by Ischemia and Reperfusion in the Myenteric Plexus. *Dig Dis Sci* 2019; **64**: 1815-1829 [PMID: 30734238 DOI: 10.1007/s10620-019-05496-8]
- 34 **Mendes CE**, Palombit K, Alves Pereira TT, Riceti Magalhães HI, Ferreira Caetano MA, Castelucci P. Effects of propenecid and brilliant blue G on rat enteric glial cells following intestinal ischemia and reperfusion. *Acta Histochem* 2023; **125**: 151985 [PMID: 36495673 DOI: 10.1016/j.acthis.2022.151985]
- 35 **Boyer L**, Ghoreishi M, Templeman V, Vallance BA, Buchan AM, Jevon G, Jacobson K. Myenteric plexus injury and apoptosis in experimental colitis. *Auton Neurosci* 2005; **117**: 41-53 [PMID: 15620569 DOI: 10.1016/j.autneu.2004.10.006]
- 36 **Sarnelli G**, De Giorgio R, Gentile F, Cali G, Grandone I, Rocco A, Cosenza V, Cuomo R, D'Argenio G. Myenteric neuronal loss in rats with experimental colitis: role of tissue transglutaminase-induced apoptosis. *Dig Liver Dis* 2009; **41**: 185-193 [PMID: 18635410 DOI: 10.1016/j.dld.2008.06.004]
- 37 **Gulbransen BD**, Bashashati M, Hirota SA, Gui X, Roberts JA, MacDonald JA, Muruve DA, McKay DM, Beck PL, Mawe GM, Thompson RJ, Sharkey KA. Activation of neuronal P2X7 receptor-pannexin-1 mediates death of enteric neurons during colitis. *Nat Med* 2012; **18**: 600-604 [PMID: 22426419 DOI: 10.1038/nm.2679]
- 38 **da Silva MV**, Marosti AR, Mendes CE, Palombit K, Castelucci P. Differential effects of experimental ulcerative colitis on

- P2X7 receptor expression in enteric neurons. *Histochem Cell Biol* 2015; **143**: 171-184 [PMID: 25201348 DOI: 10.1007/s00418-014-1270-6]
- 39 **da Silva MV**, Marosti AR, Mendes CE, Palombit K, Castelucci P. Submucosal neurons and enteric glial cells expressing the P2X7 receptor in rat experimental colitis. *Acta Histochem* 2017; **119**: 481-494 [PMID: 28501138 DOI: 10.1016/j.acthis.2017.05.001]
- 40 **Evangelinellis MM**, Souza RF, Mendes CE, Castelucci P. Effects of a P2X7 receptor antagonist on myenteric neurons in the distal colon of an experimental rat model of ulcerative colitis. *Histochem Cell Biol* 2022; **157**: 65-81 [PMID: 34626216 DOI: 10.1007/s00418-021-02039-z]
- 41 **Wright SC**, Schellenberger U, Wang H, Kinder DH, Talhouk JW, Larrick JW. Activation of CPP32-like proteases is not sufficient to trigger apoptosis: inhibition of apoptosis by agents that suppress activation of AP24, but not CPP32-like activity. *J Exp Med* 1997; **186**: 1107-1117 [PMID: 9314559 DOI: 10.1084/jem.186.7.1107]
- 42 **Jäättelä M**, Wissing D, Kokholm K, Kallunki T, Egeblad M. Hsp70 exerts its anti-apoptotic function downstream of caspase-3-like proteases. *EMBO J* 1998; **17**: 6124-6134 [PMID: 9799222 DOI: 10.1093/emboj/17.21.6124]
- 43 **Harvey KJ**, Lukovic D, Ucker DS. Caspase-dependent Cdk activity is a requisite effector of apoptotic death events. *J Cell Biol* 2000; **148**: 59-72 [PMID: 10629218 DOI: 10.1083/jcb.148.1.59]
- 44 **Uesaka T**, Jain S, Yonemura S, Uchiyama Y, Milbrandt J, Enomoto H. Conditional ablation of GFRalpha1 in postmigratory enteric neurons triggers unconventional neuronal death in the colon and causes a Hirschsprung's disease phenotype. *Development* 2007; **134**: 2171-2181 [PMID: 17507417 DOI: 10.1242/dev.001388]
- 45 **Fricke M**, Tolkovsky AM, Borutaite V, Coleman M, Brown GC. Neuronal Cell Death. *Physiol Rev* 2018; **98**: 813-880 [PMID: 29488822 DOI: 10.1152/physrev.00011.2017]
- 46 **Galluzzi L**, Vitale I, Aaronson SA, Abrams JM, Adam D, Agostinis P, Alnemri ES, Altucci L, Amelio I, Andrews DW, Annicchiarico-Petruzzelli M, Antonov AV, Arama E, Baehrecke EH, Barlev NA, Bazan NG, Bernassola F, Bertrand MJM, Bianchi K, Blagosklonny MV, Blomgren K, Borner C, Boya P, Brenner C, Campanella M, Candi E, Carmona-Gutierrez D, Cecconi F, Chan FK, Chandel NS, Cheng EH, Chipuk JE, Cidlowski JA, Ciechanover A, Cohen GM, Conrad M, Cubillos-Ruiz JR, Czabotar PE, D'Angiolella V, Dawson TM, Dawson VL, De Laurenzi V, De Maria R, Debatin KM, DeBerardinis RJ, Deshmukh M, Di Daniele N, Di Virgilio F, Dixit VM, Dixon SJ, Duckett CS, Dynlacht BD, El-Deiry WS, Elrod JW, Fimia GM, Fulda S, Garcia-Sáez AJ, Garg AD, Garrido C, Gavathiotis E, Golstein P, Gottlieb E, Green DR, Greene LA, Gronemeyer H, Gross A, Hajnoczky G, Hardwick JM, Harris IS, Hengartner MO, Hetz C, Ichijo H, Jäättelä M, Joseph B, Jost PJ, Juin PP, Kaiser WJ, Karin M, Kaufmann T, Kepp O, Kimchi A, Kitsis RN, Klionsky DJ, Knight RA, Kumar S, Lee SW, Lemasters JJ, Levine B, Linkermann A, Lipton SA, Lockshin RA, López-Otín C, Lowe SW, Luedde T, Lugli E, MacFarlane M, Madeo F, Malewicz M, Malorni W, Manic G, Marine JC, Martin SJ, Martinou JC, Medema JP, Mehlen P, Meier P, Melino S, Miao EA, Molkenin JD, Moll UM, Muñoz-Pinedo C, Nagata S, Nuñez G, Oberst A, Oren M, Overholtzer M, Pagano M, Panaretakis T, Pasparakis M, Penninger JM, Pereira DM, Pervaiz S, Peter ME, Piacentini M, Pinton P, Prehn JHM, Puthalakath H, Rabinovich GA, Rehm M, Rizzuto R, Rodrigues CMP, Rubinsztein DC, Rudel T, Ryan KM, Sayan E, Scorrano L, Shao F, Shi Y, Silke J, Simon HU, Sistigu A, Stockwell BR, Strasser A, Szabadkai G, Tait SWG, Tang D, Tavernarakis N, Thorburn A, Tsjimoto Y, Turk B, Vanden Berghe T, Vandenabeele P, Vander Heiden MG, Villunger A, Virgin HW, Vousden KH, Vucic D, Wagner EF, Walczak H, Wallach D, Wang Y, Wells JA, Wood Y, Yuan J, Zakeri Z, Zhivotovskiy B, Zitvogel L, Melino G, Kroemer G. Molecular mechanisms of cell death: recommendations of the Nomenclature Committee on Cell Death 2018. *Cell Death Differ* 2018; **25**: 486-541 [PMID: 29362479 DOI: 10.1038/s41418-017-0012-4]
- 47 **Kopp R**, Krautloher A, Ramírez-Fernández A, Nicke A. P2X7 Interactions and Signaling - Making Head or Tail of It. *Front Mol Neurosci* 2019; **12**: 183 [PMID: 31440138 DOI: 10.3389/fnmol.2019.00183]
- 48 **Volonté C**, Amadio S, Cavaliere F, D'Ambrosi N, Vacca F, Bernardi G. Extracellular ATP and neurodegeneration. *Curr Drug Targets CNS Neurol Disord* 2003; **2**: 403-412 [PMID: 14683468 DOI: 10.2174/1568007033482643]
- 49 **Franke H**, Illes P. Involvement of P2 receptors in the growth and survival of neurons in the CNS. *Pharmacol Ther* 2006; **109**: 297-324 [PMID: 16102837 DOI: 10.1016/j.pharmthera.2005.06.002]
- 50 **Franke H**, Verkhatsky A, Burnstock G, Illes P. Pathophysiology of astroglial purinergic signalling. *Purinergic Signal* 2012; **8**: 629-657 [PMID: 22544529 DOI: 10.1007/s11302-012-9300-0]
- 51 **Roberts JA**, Lukewich MK, Sharkey KA, Furness JB, Mawe GM, Lomax AE. The roles of purinergic signaling during gastrointestinal inflammation. *Curr Opin Pharmacol* 2012; **12**: 659-666 [PMID: 23063457 DOI: 10.1016/j.coph.2012.09.011]
- 52 **Marques CC**, Castelo-Branco MT, Pacheco RG, Buongusto F, do Rosário A Jr, Schanaider A, Coutinho-Silva R, de Souza HS. Prophylactic systemic P2X7 receptor blockade prevents experimental colitis. *Biochim Biophys Acta* 2014; **1842**: 65-78 [PMID: 24184714 DOI: 10.1016/j.bbadis.2013.10.012]
- 53 **Ohishi A**, Keno Y, Marumiya A, Sudo Y, Uda Y, Matsuda K, Morita Y, Furuta T, Nishida K, Nagasawa K. Expression level of P2X7 receptor is a determinant of ATP-induced death of mouse cultured neurons. *Neuroscience* 2016; **319**: 35-45 [PMID: 26812038 DOI: 10.1016/j.neuroscience.2016.01.048]
- 54 **Di Virgilio F**, Dal Ben D, Sarti AC, Giuliani AL, Falzoni S. The P2X7 Receptor in Infection and Inflammation. *Immunity* 2017; **47**: 15-31 [PMID: 28723547 DOI: 10.1016/j.immuni.2017.06.020]
- 55 **Zhang WJ**, Zhu ZM, Liu ZX. The role and pharmacological properties of the P2X7 receptor in neuropathic pain. *Brain Res Bull* 2020; **155**: 19-28 [PMID: 31778766 DOI: 10.1016/j.brainresbull.2019.11.006]
- 56 **Wan P**, Liu X, Xiong Y, Ren Y, Chen J, Lu N, Guo Y, Bai A. Extracellular ATP mediates inflammatory responses in colitis via P2 × 7 receptor signaling. *Sci Rep* 2016; **6**: 19108 [PMID: 26739809 DOI: 10.1038/srep19108]
- 57 **Burnstock G**, Jacobson KA, Christofi FL. Purinergic drug targets for gastrointestinal disorders. *Curr Opin Pharmacol* 2017; **37**: 131-141 [PMID: 29149731 DOI: 10.1016/j.coph.2017.10.011]
- 58 **Cheng N**, Zhang L, Liu L. Understanding the Role of Purinergic P2X7 Receptors in the Gastrointestinal System: A Systematic Review. *Front Pharmacol* 2021; **12**: 786579 [PMID: 34987401 DOI: 10.3389/fphar.2021.786579]
- 59 **Mishra A**, Behura A, Kumar A, Naik L, Swain A, Das M, Sarangi SS, Dokania P, Dirisala VR, Bhutia SK, Mishra A, Singh R, Dhiman R. P2X7 receptor in multifaceted cellular signalling and its relevance as a potential therapeutic target in

- different diseases. *Eur J Pharmacol* 2021; **906**: 174235 [PMID: 34097884 DOI: 10.1016/j.ejphar.2021.174235]
- 60 **Antonoli L**, Giron MC, Colucci R, Pellegrini C, Sacco D, Caputi V, Orso G, Tuccori M, Scarpignato C, Blandizzi C, Fornai M. Involvement of the P2X7 purinergic receptor in colonic motor dysfunction associated with bowel inflammation in rats. *PLoS One* 2014; **9**: e116253 [PMID: 25549098 DOI: 10.1371/journal.pone.0116253]
- 61 **Liu Y**, Liu X. Research progress of P2X7 receptor in inflammatory bowel disease. *Scand J Gastroenterol* 2019; **54**: 521-527 [PMID: 31056977 DOI: 10.1080/00365521.2019.1609077]
- 62 **Souza RF**, Evangelinellis MM, Mendes CE, Righetti M, Lourenço MCS, Castelucci P. P2X7 receptor antagonist recovers ileum myenteric neurons after experimental ulcerative colitis. *World J Gastrointest Pathophysiol* 2020; **11**: 84-103 [PMID: 32587788 DOI: 10.4291/wjgp.v11.i4.84]
- 63 **Magalhães HIR**, Castelucci P. Enteric nervous system and inflammatory bowel diseases: Correlated impacts and therapeutic approaches through the P2X7 receptor. *World J Gastroenterol* 2021; **27**: 7909-7924 [PMID: 35046620 DOI: 10.3748/wjg.v27.i46.7909]
- 64 **Cooper HS**, Murthy SN, Shah RS, Sedergran DJ. Clinicopathologic study of dextran sulfate sodium experimental murine colitis. *Lab Invest* 1993; **69**: 238-249 [PMID: 8350599]
- 65 **Hoffmann M**, Schwertassek U, Seydel A, Weber K, Falk W, Hauschildt S, Lehmann J. A refined and translationally relevant model of chronic DSS colitis in BALB/c mice. *Lab Anim* 2018; **52**: 240-252 [PMID: 29192559 DOI: 10.1177/0023677217742681]
- 66 **Wallace JL**, Keenan CM. An orally active inhibitor of leukotriene synthesis accelerates healing in a rat model of colitis. *Am J Physiol* 1990; **258**: G527-G534 [PMID: 1970708 DOI: 10.1152/ajpgi.1990.258.4.G527]
- 67 **Fabia R**, Ar'Rajab A, Johansson ML, Willén R, Andersson R, Molin G, Bengmark S. The effect of exogenous administration of *Lactobacillus reuteri* R2LC and oat fiber on acetic acid-induced colitis in the rat. *Scand J Gastroenterol* 1993; **28**: 155-162 [PMID: 8382837 DOI: 10.3109/00365529309096063]
- 68 **Vieira C**, Ferreirinha F, Magalhães-Cardoso MT, Silva I, Marques P, Correia-de-Sá P. Post-inflammatory Ileitis Induces Non-neuronal Purinergic Signaling Adjustments of Cholinergic Neurotransmission in the Myenteric Plexus. *Front Pharmacol* 2017; **8**: 811 [PMID: 29167643 DOI: 10.3389/fphar.2017.00811]
- 69 **Orechio D**, Andrade Aguiar B, Baroni Diniz G, Cioni Bittencourt J, Haemmerle CAS, Watanabe IS, Miglino MA, Castelucci P. Morphological and Cellular Characterization of the Fetal Canine (*Canis lupus familiaris*) Subventricular Zone, Rostral Migratory Stream, and Olfactory Bulb. *Anat Rec (Hoboken)* 2018; **301**: 1570-1584 [PMID: 29752870 DOI: 10.1002/ar.23855]
- 70 **Sant'Ana DM**, Góis MB, Zanoni JN, da Silva AV, da Silva CJ, Araújo EJ. Intraepithelial lymphocytes, goblet cells and VIP-IR submucosal neurons of jejunum rats infected with *Toxoplasma gondii*. *Int J Exp Pathol* 2012; **93**: 279-286 [PMID: 22804764 DOI: 10.1111/j.1365-2613.2012.00824.x]
- 71 **Góis MB**, Hermes-Uliana C, Barreto Zago MC, Zanoni JN, da Silva AV, de Miranda-Neto MH, de Almeida Araújo EJ, Sant'Ana Dde M. Chronic infection with *Toxoplasma gondii* induces death of submucosal enteric neurons and damage in the colonic mucosa of rats. *Exp Parasitol* 2016; **164**: 56-63 [PMID: 26902605 DOI: 10.1016/j.exppara.2016.02.009]
- 72 **Pavanelli MF**, Colli CM, Gomes ML, Góis MB, de Alcântara Nogueira de Melo G, de Almeida Araújo EJ, de Mello Gonçalves Sant'Ana D. Comparative study of effects of assemblages AII and BIV of *Giardia duodenalis* on mucosa and microbiota of the small intestine in mice. *Biomed Pharmacother* 2018; **101**: 563-571 [PMID: 29514129 DOI: 10.1016/j.biopha.2018.02.141]
- 73 **Furlan-Murari PJ**, de Lima ECS, de Souza FP, Urrea-Rojas AM, Eugenio Pupim AC, de Almeida Araújo EJ, Meletti PC, Seino Leal CN, Fernandes LL, Lopera-Barrero NM. Inclusion of  $\beta$ -1,3/1,6-glucan in the ornamental fish, Jewel tetra (*Hyphessobrycon eques*), and its effects on growth, blood glucose, and intestinal histology. *Aquacult Int* 2022; **30**: 501-515 [DOI: 10.1007/s10499-021-00815-1]
- 74 **Ke P**, Shao BZ, Xu ZQ, Chen XW, Liu C. Intestinal Autophagy and Its Pharmacological Control in Inflammatory Bowel Disease. *Front Immunol* 2016; **7**: 695 [PMID: 28119697 DOI: 10.3389/fimmu.2016.00695]
- 75 **Ishisono K**, Mano T, Yabe T, Kitaguchi K. Dietary Fiber Pectin Ameliorates Experimental Colitis in a Neutral Sugar Side Chain-Dependent Manner. *Front Immunol* 2019; **10**: 2979 [PMID: 31921214 DOI: 10.3389/fimmu.2019.02979]
- 76 **Arseneau KO**, Tamagawa H, Pizarro TT, Cominelli F. Innate and adaptive immune responses related to IBD pathogenesis. *Curr Gastroenterol Rep* 2007; **9**: 508-512 [PMID: 18377804 DOI: 10.1007/s11894-007-0067-3]
- 77 **Frank DN**, St Amand AL, Feldman RA, Boedeker EC, Harpaz N, Pace NR. Molecular-phylogenetic characterization of microbial community imbalances in human inflammatory bowel diseases. *Proc Natl Acad Sci U S A* 2007; **104**: 13780-13785 [PMID: 17699621 DOI: 10.1073/pnas.0706625104]
- 78 **Neurath MF**. Host-microbiota interactions in inflammatory bowel disease. *Nat Rev Gastroenterol Hepatol* 2020; **17**: 76-77 [PMID: 31848474 DOI: 10.1038/s41575-019-0248-1]
- 79 **Tavakoli P**, Vollmer-Conna U, Hadzi-Pavlovic D, Grimm MC. A Review of Inflammatory Bowel Disease: A Model of Microbial, Immune and Neuropsychological Integration. *Public Health Rev* 2021; **42**: 1603990 [PMID: 34692176 DOI: 10.3389/phrs.2021.1603990]
- 80 **Caetano MAF**, Castelucci P. Role of short chain fatty acids in gut health and possible therapeutic approaches in inflammatory bowel diseases. *World J Clin Cases* 2022; **10**: 9985-10003 [PMID: 36246826 DOI: 10.12998/wjcc.v10.i28.9985]
- 81 **Sanovic S**, Lamb DP, Blennerhassett MG. Damage to the enteric nervous system in experimental colitis. *Am J Pathol* 1999; **155**: 1051-1057 [PMID: 10514387 DOI: 10.1016/S0002-9440(10)65207-8]
- 82 **Cirillo C**, Sarnelli G, Cuomo R. Enteric nervous system abnormalities in ulcerative colitis. In: O'Connor MB. *Ulcerative Colitis-Epidemiology, Pathogenesis and Complications*. 2011. [cited 20 March 2023]. Available from: [https://cdn.intechopen.com/pdfs/24837/InTech-Enteric\\_nervous\\_system\\_abnormalities\\_in\\_ulcerative\\_colitis.pdf](https://cdn.intechopen.com/pdfs/24837/InTech-Enteric_nervous_system_abnormalities_in_ulcerative_colitis.pdf)
- 83 **Figliuolo VR**, Savio LEB, Safya H, Nanini H, Bernardazzi C, Abalo A, de Souza HSP, Kanellopoulos J, Bobé P, Coutinho CMLM, Coutinho-Silva R. P2X7 receptor promotes intestinal inflammation in chemically induced colitis and triggers death of mucosal regulatory T cells. *Biochim Biophys Acta Mol Basis Dis* 2017; **1863**: 1183-1194 [PMID: 28286160 DOI: 10.1016/j.bbdis.2017.03.004]

- 84 **Spear ET**, Mawe GM. Enteric neuroplasticity and dysmotility in inflammatory disease: key players and possible therapeutic targets. *Am J Physiol Gastrointest Liver Physiol* 2019; **317**: G853-G861 [PMID: 31604034 DOI: 10.1152/ajpgi.00206.2019]
- 85 **Stavelly R**, Abalo R, Nurgali K. Targeting Enteric Neurons and Plexitis for the Management of Inflammatory Bowel Disease. *Curr Drug Targets* 2020; **21**: 1428-1439 [PMID: 32416686 DOI: 10.2174/1389450121666200516173242]
- 86 **Brenna Ø**, Furnes MW, Drozdov I, van Beelen Granlund A, Flatberg A, Sandvik AK, Zwiggelaar RT, Mårvik R, Nordrum IS, Kidd M, Gustafsson BI. Relevance of TNBS-colitis in rats: a methodological study with endoscopic, histologic and Transcriptomic [corrected] characterization and correlation to IBD. *PLoS One* 2013; **8**: e54543 [PMID: 23382912 DOI: 10.1371/journal.pone.0054543]
- 87 **Morris GP**, Beck PL, Herridge MS, Depew WT, Szewczuk MR, Wallace JL. Hapten-induced model of chronic inflammation and ulceration in the rat colon. *Gastroenterology* 1989; **96**: 795-803 [PMID: 2914642]
- 88 **Kawada M**, Arihiro A, Mizoguchi E. Insights from advances in research of chemically induced experimental models of human inflammatory bowel disease. *World J Gastroenterol* 2007; **13**: 5581-5593 [PMID: 17948932 DOI: 10.3748/wjg.v13.i42.5581]
- 89 **Sigalet DL**, Wallace L, De Heuval E, Sharkey KA. The effects of glucagon-like peptide 2 on enteric neurons in intestinal inflammation. *Neurogastroenterol Motil* 2010; **22**: 1318-e350 [PMID: 20718942 DOI: 10.1111/j.1365-2982.2010.01585.x]
- 90 **Chassaing B**, Aitken JD, Malleshappa M, Vijay-Kumar M. Dextran sulfate sodium (DSS)-induced colitis in mice. *Curr Protoc Immunol* 2014; **104**: 15.25.1-15.25.14 [PMID: 24510619 DOI: 10.1002/0471142735.im1525s104]
- 91 **Wirtz S**, Neufert C, Weigmann B, Neurath MF. Chemically induced mouse models of intestinal inflammation. *Nat Protoc* 2007; **2**: 541-546 [PMID: 17406617 DOI: 10.1038/nprot.2007.41]
- 92 **Silva I**, Pinto R, Mateus V. Preclinical Study in Vivo for New Pharmacological Approaches in Inflammatory Bowel Disease: A Systematic Review of Chronic Model of TNBS-Induced Colitis. *J Clin Med* 2019; **8** [PMID: 31581545 DOI: 10.3390/jcm8101574]
- 93 **Neves AR**, Castelo-Branco MT, Figliuolo VR, Bernardazzi C, Buongusto F, Yoshimoto A, Nanini HF, Coutinho CM, Carneiro AJ, Coutinho-Silva R, de Souza HS. Overexpression of ATP-activated P2X7 receptors in the intestinal mucosa is implicated in the pathogenesis of Crohn's disease. *Inflamm Bowel Dis* 2014; **20**: 444-457 [PMID: 24412990 DOI: 10.1097/01.MIB.0000441201.10454.06]
- 94 **Hofman P**, Cherfils-Vicini J, Bazin M, Ilie M, Juhel T, Hébuterne X, Gilson E, Schmid-Alliana A, Boyer O, Adriouch S, Vouret-Craviari V. Genetic and pharmacological inactivation of the purinergic P2RX7 receptor dampens inflammation but increases tumor incidence in a mouse model of colitis-associated cancer. *Cancer Res* 2015; **75**: 835-845 [PMID: 25564520 DOI: 10.1158/0008-5472.CAN-14-1778]
- 95 **Linden DR**, Couvrette JM, Ciolino A, McQuoid C, Blaszyk H, Sharkey KA, Mawe GM. Indiscriminate loss of myenteric neurones in the TNBS-inflamed guinea-pig distal colon. *Neurogastroenterol Motil* 2005; **17**: 751-760 [PMID: 16185315 DOI: 10.1111/j.1365-2982.2005.00703.x]
- 96 **Poli E**, Lazzaretti M, Grandi D, Pozzoli C, Coruzzi G. Morphological and functional alterations of the myenteric plexus in rats with TNBS-induced colitis. *Neurochem Res* 2001; **26**: 1085-1093 [PMID: 11699935 DOI: 10.1023/a:1012313424144]
- 97 **Ziegler U**, Groscurth P. Morphological features of cell death. *News Physiol Sci* 2004; **19**: 124-128 [PMID: 15143207 DOI: 10.1152/nips.01519.2004]
- 98 **Elmore S**. Apoptosis: a review of programmed cell death. *Toxicol Pathol* 2007; **35**: 495-516 [PMID: 17562483 DOI: 10.1080/01926230701320337]
- 99 **Degterev A**, Yuan J. Expansion and evolution of cell death programmes. *Nat Rev Mol Cell Biol* 2008; **9**: 378-390 [PMID: 18414491 DOI: 10.1038/nrm2393]
- 100 **Poon IK**, Lucas CD, Rossi AG, Ravichandran KS. Apoptotic cell clearance: basic biology and therapeutic potential. *Nat Rev Immunol* 2014; **14**: 166-180 [PMID: 24481336 DOI: 10.1038/nri3607]
- 101 **Ponder KG**, Boise LH. The prodomain of caspase-3 regulates its own removal and caspase activation. *Cell Death Discov* 2019; **5**: 56 [PMID: 30701088 DOI: 10.1038/s41420-019-0142-1]
- 102 **Lister MF**, Sharkey J, Sawatzky DA, Hodgkiss JP, Davidson DJ, Rossi AG, Finlayson K. The role of the purinergic P2X7 receptor in inflammation. *J Inflamm (Lond)* 2007; **4**: 5 [PMID: 17367517 DOI: 10.1186/1476-9255-4-5]
- 103 **Antonoli L**, Colucci R, Pellegrini C, Giustarini G, Tuccori M, Blandizzi C, Fornai M. The role of purinergic pathways in the pathophysiology of gut diseases: pharmacological modulation and potential therapeutic applications. *Pharmacol Ther* 2013; **139**: 157-188 [PMID: 23588157 DOI: 10.1016/j.pharmthera.2013.04.002]
- 104 **Rotondo JC**, Mazziotta C, Lanzillotti C, Stefani C, Badiale G, Campione G, Martini F, Tognon M. The Role of Purinergic P2X7 Receptor in Inflammation and Cancer: Novel Molecular Insights and Clinical Applications. *Cancers (Basel)* 2022; **14** [PMID: 35267424 DOI: 10.3390/cancers14051116]
- 105 **North RA**. Molecular physiology of P2X receptors. *Physiol Rev* 2002; **82**: 1013-1067 [PMID: 12270951 DOI: 10.1152/physrev.00015.2002]
- 106 **Burnstock G**. Purine and pyrimidine receptors. *Cell Mol Life Sci* 2007; **64**: 1471-1483 [PMID: 17375261 DOI: 10.1007/s00018-007-6497-0]
- 107 **Dubyak GR**. P2X7 receptor regulation of non-classical secretion from immune effector cells. *Cell Microbiol* 2012; **14**: 1697-1706 [PMID: 22882764 DOI: 10.1111/cmi.12001]
- 108 **Neurath MF**, Pettersson S, Meyer zum Büschenfelde KH, Strober W. Local administration of antisense phosphorothioate oligonucleotides to the p65 subunit of NF-kappa B abrogates established experimental colitis in mice. *Nat Med* 1996; **2**: 998-1004 [PMID: 8782457 DOI: 10.1038/nm0996-998]
- 109 **Schreiber S**, Nikolaus S, Hampe J. Activation of nuclear factor kappa B inflammatory bowel disease. *Gut* 1998; **42**: 477-484 [PMID: 9616307 DOI: 10.1136/gut.42.4.477]
- 110 **Lawrance IC**, Wu F, Leite AZ, Willis J, West GA, Fiocchi C, Chakravarti S. A murine model of chronic inflammation-induced intestinal fibrosis down-regulated by antisense NF-kappa B. *Gastroenterology* 2003; **125**: 1750-1761 [PMID: 14724828 DOI: 10.1053/j.gastro.2003.08.027]

- 111 **Atreya I**, Atreya R, Neurath MF. NF-kappaB in inflammatory bowel disease. *J Intern Med* 2008; **263**: 591-596 [PMID: 18479258 DOI: 10.1111/j.1365-2796.2008.01953.x]
- 112 **Listwak SJ**, Rathore P, Herkenham M. Minimal NF-κB activity in neurons. *Neuroscience* 2013; **250**: 282-299 [PMID: 23872390 DOI: 10.1016/j.neuroscience.2013.07.013]
- 113 **Peyrin-Biroulet L**, Bressenot A, Kampman W. Histologic remission: the ultimate therapeutic goal in ulcerative colitis? *Clin Gastroenterol Hepatol* 2014; **12**: 929-34.e2 [PMID: 23911875 DOI: 10.1016/j.cgh.2013.07.022]
- 114 **Chateau T**, Feakins R, Marchal-Bressenot A, Magro F, Danese S, Peyrin-Biroulet L. Histological Remission in Ulcerative Colitis: Under the Microscope Is the Cure. *Am J Gastroenterol* 2020; **115**: 179-189 [PMID: 31809296 DOI: 10.14309/ajg.0000000000000437]
- 115 **Udawat H**, Nunia V, Mathur P, Udawat HP, Gaur KL, Saxena AK, Mohan MK. Histopathological and Immunohistochemical Findings in Congenital Pouch Colon: A Prospective Study. *Pathobiology* 2017; **84**: 202-209 [PMID: 28605747 DOI: 10.1159/000460821]
- 116 **Xu X**, Lin S, Yang Y, Gong X, Tong J, Li K, Li Y. Histological and ultrastructural changes of the colon in dextran sodium sulfate-induced mouse colitis. *Exp Ther Med* 2020; **20**: 1987-1994 [PMID: 32782508 DOI: 10.3892/etm.2020.8946]
- 117 **Kim YS**, Ho SB. Intestinal goblet cells and mucins in health and disease: recent insights and progress. *Curr Gastroenterol Rep* 2010; **12**: 319-330 [PMID: 20703838 DOI: 10.1007/s11894-010-0131-2]
- 118 **McCauley HA**, Guasch G. Three cheers for the goblet cell: maintaining homeostasis in mucosal epithelia. *Trends Mol Med* 2015; **21**: 492-503 [PMID: 26144290 DOI: 10.1016/j.molmed.2015.06.003]
- 119 **Parikh K**, Antanaviciute A, Fawcner-Corbett D, Jagielowicz M, Aulicino A, Lagerholm C, Davis S, Kinchen J, Chen HH, Alham NK, Ashley N, Johnson E, Hublitz P, Bao L, Lukomska J, Andev RS, Björklund E, Kessler BM, Fischer R, Goldin R, Koohy H, Simmons A. Colonic epithelial cell diversity in health and inflammatory bowel disease. *Nature* 2019; **567**: 49-55 [PMID: 30814735 DOI: 10.1038/s41586-019-0992-y]
- 120 **Pu Z**, Che Y, Zhang W, Sun H, Meng T, Xie H, Cao L, Hao H. Dual roles of IL-18 in colitis through regulation of the function and quantity of goblet cells. *Int J Mol Med* 2019; **43**: 2291-2302 [PMID: 31017261 DOI: 10.3892/ijmm.2019.4156]
- 121 **Van der Sluis M**, De Koning BA, De Bruijn AC, Velcich A, Meijerink JP, Van Goudoever JB, Büller HA, Dekker J, Van Seuningen I, Renes IB, Einerhand AW. Muc2-deficient mice spontaneously develop colitis, indicating that MUC2 is critical for colonic protection. *Gastroenterology* 2006; **131**: 117-129 [PMID: 16831596 DOI: 10.1053/j.gastro.2006.04.020]
- 122 **Vergnolle N**, Cirillo C. Neurons and Glia in the Enteric Nervous System and Epithelial Barrier Function. *Physiology (Bethesda)* 2018; **33**: 269-280 [PMID: 29897300 DOI: 10.1152/physiol.00009.2018]
- 123 **Grondin JA**, Kwon YH, Far PM, Haq S, Khan WI. Mucins in Intestinal Mucosal Defense and Inflammation: Learning From Clinical and Experimental Studies. *Front Immunol* 2020; **11**: 2054 [PMID: 33013869 DOI: 10.3389/fimmu.2020.02054]
- 124 **Niv Y**. Mucin gene expression in the intestine of ulcerative colitis patients: a systematic review and meta-analysis. *Eur J Gastroenterol Hepatol* 2016; **28**: 1241-1245 [PMID: 27442499 DOI: 10.1097/MEG.0000000000000707]



Published by **Baishideng Publishing Group Inc**  
7041 Koll Center Parkway, Suite 160, Pleasanton, CA 94566, USA

**Telephone:** +1-925-3991568

**E-mail:** [bpgoffice@wjgnet.com](mailto:bpgoffice@wjgnet.com)

**Help Desk:** <https://www.f6publishing.com/helpdesk>

<https://www.wjgnet.com>

